Neuropharmacology 266 (2025) 110265

Contents lists available at ScienceDirect

Neuropharmacology

journal homepage: www.elsevier.com/locate/neuropharm

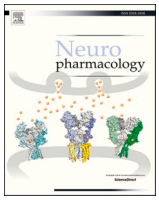

Acute kappa opioid receptor blocking disrupts the pro-cognitive effect of cannabidiol in neuropathic rats

Serena Boccella [a,*], Antimo Fusco [a], Federica Ricciardi [a], Andrea Maria Morace [a], Roozbe Bonsale [a], Michela Perrone [a], Ida Marabese [a], Danilo De Gregorio [b,c], Carmela Belardo [a], Luca Posa [d], Laura Rullo [e], Fabiana Piscitelli [f], Vincenzo di Marzo [f,g,h,i], Alessandro Nicois [f,m], Brenda Marfella [f,l], Luigia Cristino [f], Livio Luongo [a], Francesca Guida [a], Sanzio Candeletti [e], Gabriella Gobbi [j,k], Patrizia Romualdi [e], Sabatino Maione [a]

[a] Department of Experimental Medicine, Division of Pharmacology, Università della Campania "L. Vanvitelli", Naples, Italy
[b] IRCCS San Raffaele Scientific Institute, Italy
[c] Vita Salute San Raffaele University, Milan, Italy
[d] Department of Biochemistry, Weill Cornell Medicine, New York, NY, USA
[e] Department of Pharmacy and Biotechnology, Alma Mater Studiorum-University of Bologna, 40126, Bologna, Italy
[f] Institute of Biomolecular Chemistry, National Research Council of Italy, Pozzuoli, NA, Italy
[g] Faculty of Medicine and Faculty of Agricultural and Food Sciences, Canada Excellence Research Chair on the Microbiome-Endocannabinoidome Axis in Metabolic Health, Université Laval, Québec City, QC, Canada
[h] Heart and Lung Research Institute of Université Laval, Québec City, QC, Canada
[i] Institute for Nutrition and Functional Foods, Centre NUTRISS, Université Laval, Québec City, QC, Canada
[j] Neurobiological Psychiatry Unit, Department of Psychiatry, McGill University, Montreal, QC, Canada
[k] Research Institute, McGill University Health Center, McGill University, Montreal, QC, Canada
[l] Department of Biology, University of Naples Federico II, 80126, Naples, Italy
[m] Department of Biomolecular Sciences, University of Urbino Carlo Bo, Urbino, Italy

ARTICLE INFO

Handling Editor: Bruno Frenguelli

Keywords:
Cannabidiol
Neuropathic pain
Kappa opioid receptor
Long term potentiation
Cognition

ABSTRACT

Cannabidiol has been shown to ameliorate neuropathic pain and its affective components. Previous studies highlighted the pharmacological interaction between the CBD and opioid system, particularly the MOR, but the understanding of the interaction between CBD and kappa opioid receptor (KOR), physiologically stimulated by the endogenous opioid dynorphin, remains elusive. We assessed the pharmacological interactions between CBD and nor-BNI, a selective KOR antagonist in a rat neuropathic pain model. We show an increase in dynorphin peptide and its KOR receptors in the hippocampus' dentate gyrus (DG) of neuropathic rats showing allodynia, and memory deficits. Consistent with these findings, neuropathic pain was associated with long-term potentiation (LTP) impairment in the entorhinal cortex-DG, also referred to as the lateral perforant pathway (LPP). Moreover, a downregulation of the endocannabinoid 2-AG and an upregulation of the cannabinoid CB1 receptors in the DG were detected in neuropathic pain animals. Either an acute KOR antagonist administration or one-week CBD treatment normalized dynorphin levels and improved affective symptoms, LTP and receptor expression, whereas only CBD showed an anti-allodynic effect. In addition, CBD normalized the SNI-induced changes in neuroplasticity as well as endocannabinoid and GABA levels in the DG. Noteworthy, the acute blockade of the KOR carried out after CBD repeated administration causes the re-installment of some neuropathic condition symptoms.

As a whole, these original results indicate a critical relationship between the adaptive changes in the hippocampus produced by CBD and the need to maintain the recovered physiological dynorphin tone to preserve the therapeutic effect of CBD in neuropathic rats.

* Corresponding author.
E-mail address: serena.boccella@unicampania.it (S. Boccella).

https://doi.org/10.1016/j.neuropharm.2024.110265
Received 8 October 2024; Received in revised form 20 November 2024; Accepted 10 December 2024
Available online 12 December 2024

1. Introduction

Cannabidiol (CBD) is a major non-psychoactive constituent of *Cannabis Sativa* with therapeutic properties in Central Nervous System (CNS) disorders, including chronic pain (Leinen et al., 2023). It has been shown to elicit antioxidant, anti-inflammatory and analgesic effects in preclinical animal models through a pleiotropic mechanism (Izzo et al., 2009). A multitude of biological targets in the brain, such as channels and neurotransmitters, have been proposed as potential molecular pathways (Mannucci et al., 2017; Saviano et al., 2021). In fact, CBD has been shown to exert a partial antagonistic or inverse agonistic activity at cannabinoid receptor types 1 (CB1R) and 2 (CB2R), although it displays a low affinity for these receptors compared to other cannabinoid compounds (De Gregorio et al., 2019; Malvestio et al., 2021).

Dynorphin, an endogenous ligand at the kappa opioid receptor (KOR), has been recently demonstrated to promote aversiveness of chronic neuropathic pain (Navratilova E. et al., 2019; Caputi et al., 2019) Additionally, KOR signaling promotes the loss of descending control of nociception in rodent models of chronic pain (Nation et al., 2018) suggesting that KOR antagonism may be useful in targeting cognitive/affective comorbidities of chronic pain. The existence of functional interaction between cannabinoid and opioid systems has been suggested in several conditions, including pain control (Desroches and Beaulieu, 2010; Ross et al., 2023; Pearl-Dowler et al., 2023). Opioids and cannabinoids bind inhibitory G protein-coupled receptors which are widely expressed within the neural antinociceptive pathways (Welch, 2009). Nevertheless, the singular stimulation of opioid or cannabinoid receptors leads to the analgesia, due the overlapping anatomical distribution and the similar intracellular signalling pathways, the bidirectional functional interaction, as well as, additive or synergistic effects have been proposed (Massotte, 2015; Scavone et al., 2013). Molecular interactions between receptors have been shown with colocalization or heterodimerization mainly for CB1 and delta or mu opioid receptors within the spinal cord, striatum, or locus coeruleus (Massotte, 2015; Scavone et al., 2013). Combination of delta-9-tetrahydrocannabinol (THC) and morphine has been shown to produce antinociception as a result of CB1 receptor-mediated release of endogenous opioid peptides (Cichewicz, 2004). In another study, the antinociceptive effects of THC, which show a mixed ability to activate both CB1 and CB2 receptors, have been attenuated by the kappa opioid receptor (KOR) antagonist, norbinaltorphimine, in arthritic rats (Cox and Welch, 2004). However, the mechanism concerning the interaction of the CBD with the KOR remains elusive.

Employing a multidisciplinary approach spanning from behavioral pharmacology, electrophysiology, morphology and neurochemical analysis, here we assessed the contribution of the opioid system in the ability of CBD to exert an analgesic effect and to revert the cognitive impairments induced by the neuropathic pain condition. To this end, we used the spared nerve injury (SNI) model which reproduces pain and related comorbidities by mimicking human experience (Guida et al., 2020, 2022). Hence, we analysed functional alterations accompanying pain symptoms by recording within the entorhinal cortex (LEC)-dentate gyrus (DG) pathway, as a key circuit controlling both sensorial and cognitive functioning. We hypothesized that an SNI-mediated increase in dynorphin levels may participate in pain-related symptoms. Thus, the involvement of KOR was investigated by injecting the nor-binaltorphimine (nor-BNI) alone or in the presence of CBD.

This study elucidates the functional interaction of opioids and cannabinoids in pain and associated maladaptive behaviours, thus providing a new picture of the cross-talk of these systems.

2. Materials and methods

2.1. Animals

Male Wistar rats weighing between 270 and 280 g (8–9-week-old) were sourced from Envigo in Italy. Animals were housed in groups of 2–3 per cage, maintained under controlled lighting conditions (12-h light: dark cycle with lights on at 06:00) and standard environmental parameters (room temperature maintained at 22 ± 1 °C, humidity at 60 ± 10%) for a minimum of one week before commencing the experiments. The rats had access to rat chow and tap water ad libitum. All experimental procedures were ethically approved by the Animal Ethics Committee of the University of Campania "Luigi Vanvitelli" and conducted in accordance with Italian Legislative Decree (D.L. 116/92) and European Commission Directive (O.J. of E.C. L358/1, 18/12/86) regulations governing the protection of laboratory animals (Protocol N° 89/2023-PR). Stringent efforts were undertaken to minimize animal discomfort and reduce the total number of animals used.

2.2. Spared nerve injury model

The neuropathic pain model known as spared nerve injury (SNI) was implemented following the procedure outlined by Decosterd and Woolf (2000). Rats were anesthetized using isoflurane (induction 4 %, maintenance 1.5 % in oxygen) and the sciatic nerve was exposed at its trifurcation into the sural, tibial, and common peroneal nerves. The tibial and common peroneal nerves were tightly ligated with 5.0 silk thread and then transected just distal to the ligation site, while the sural nerve remained intact. Sham-operated rats underwent anesthesia and exposure of the sciatic nerve at the same level, without ligation. The SNI model is recognized for its consistent induction of neuropathic pain, characterized by alterations in neuronal firing patterns at both spinal and supraspinal levels (Boccella et al., 2015; Palazzo et al., 2013), as well as deficits in affective and cognitive behavior akin to advanced neuropathy in humans (Rahn et al., 2013). Mechanical hypersensitivity typically manifests four days post-surgery and stabilizes between seven to ten days post-surgery (Decosterd and Woolf, 2000).

2.3. Mechanical allodynia

The von Frey test apparatus (Ugo Basile, Italy) was utilized to measure the nociceptive threshold to mechanical stimuli. This apparatus employs a series of nylon monofilaments with varying thicknesses, each exerting different levels of force when applied to the glabrous area of the paw. Through this method, researchers can determine the force required to elicit paw withdrawal responses (Meunier et al., 2005; Ren and Dubner, 1999). Rats were individually placed in acrylic boxes measuring 23 × 20 × 18 cm, positioned on a non-malleable 5 mm^2 steel mesh table. This setup allowed stimulation to be delivered through the mesh using the tip of a von Frey test rod, targeting the center of the plantar surface of the hind paw of each rat until a withdrawal response was observed. Prior to testing, rats underwent a habituation period lasting 15–30 min in the experimental environment to minimize stress-related behaviors. Stimulation was applied to the glabrous surfaces of both hind paws, both ipsilateral and contralateral to the chronic lesion of the sciatic nerve.

2.4. Novel object recognition (NOR) test

The NOR test was performed as previously described (Tucci et al., 2014). Briefly, the experimental protocol includes a training and a test trial that were interspersed by a 24-h intersession period. In the training trial (T1), animals received a 10-min exposure to two identical objects placed in the centre of the experimental arena. Then, during the test phase (T2, 10 min), one of the familiar objects (F) was substituted with a novel differently designed object (N), without changing the configuration in the arena. Throughout the experimental procedure, objects and their relative position were counterbalanced and randomly permuted. After each trial, arena and objects were cleaned with a 50% ethanol solution and dried to avoid the presence of olfactory cues. The discrimination index was evaluated and graphically presented in results, expressed as ratio between the difference in time spent exploring the

novel object (Tn–Tf) over the total amount of exploration time (DI = Tn–Tf/Tn + Tf).

2.5. In vivo recording of hippocampal long-term potentiation (LTP)

Rats were first anesthetized with urethane (1.5 g/kg, i.p.) and fixed in a stereotaxic table (Stoelting Co USA) for inserting the stimulating and the recording electrodes in the lateral entorhinal cortex (LEC) and dentate gyrus (DG), respectively, following the coordinates from Paxinos and Watson atlas brain: [AP = -7.2 from bregma, ML = 4.0 and DV = 2.3 mm for LEC] and [AP = −3.5 mm from bregma, ML = 2.25 and DV = 2.5 mm for DG]. The stimulating and recording electrodes were slowly lowered at the selected positions until a field excitatory postsynaptic potential (fEPSP) appeared, induced by test pulses (0.2 ms in duration) delivered at the frequency of 0.033 Hz. After those responses stabilized, a 30 min stable baseline was recorded. Following baseline recording, a high frequency stimulation (TBS) consisting of 6 trains, 6 bursts, 6 pulses a 400 Hz, interburst interval: 200 ms, intertrain interval: 20 s, was applied to LEC for the induction of LTP, as shown in the graphical representation in Fig. 1D. After TBS, the recording of the baseline fEPSPs continued for 90 min. The induction of LTP was successful if the amplitude and the slope of fEPSPs increased more than 20% for at least 30 min after the TBS (2, 3). To obtain fEPSP slope values, the region of interest was set from peak-to-peak and the software (WinLTP 2.30, Bristo, UK), calculated the average slope within 10–90% of this region.

2.6. In vivo microdialysis

Microdialysis experiments were conducted in conscious, freely moving rats. Initially, rats were anesthetized with a combination of ketamine (50 mg/kg) and medetomidine (2 mg/kg) administered intraperitoneally (i.p.). Subsequently, they were stereotaxically implanted with concentric microdialysis probes targeting the Dentate Gyrus (DG) at the following coordinates: AP: 4.1 mm from bregma, ML: 1.5 mm from midline, and DV: 3.5 mm below the dura mater (Zamberletti et al., 2017). The dialysis probes were constructed using 25 G stainless steel tubing (0.3 mm inner diameter, 0.5 mm outer diameter) from A-M Systems, Sequim, WA, with inlet and outlet cannulae (0.04 mm inner diameter, 0.14 mm outer diameter) made of fused silica tubing (Scientific Glass Engineering) coated with a dialysis membrane (Enka AG, Wuppertal, Germany). Following a 24-h recovery period, dialysis commenced by perfusing the implants with artificial cerebrospinal fluid (ACSF) containing NaCl (147 mM), CaCl2 (2.2 mM), and KCl (4 mM) at a rate of 1 μL/min using a Harvard Apparatus infusion pump. After a 60-min equilibration period, baseline dialysate samples were collected in 30-min intervals over 7 consecutive sessions. Subsequently, Norbinaltorphimine (nor-BNI) was injected intraperitoneally (i.p.), and

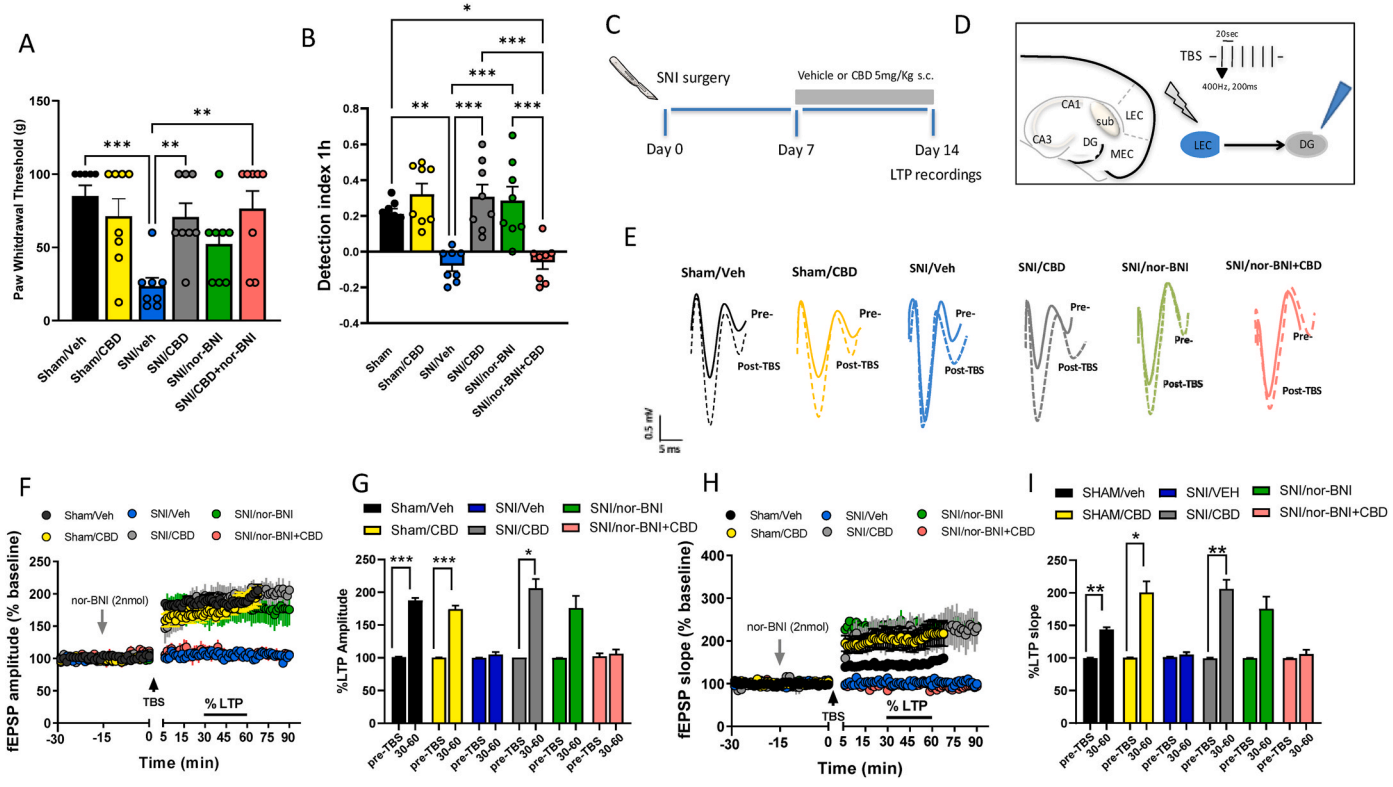

Fig. 1. Effect of CBD or nor-BNI on pain and, cognitive functioning in SNI rats "A" shows the paw withdrawal threshold (grams) in the Von Frey test, "B" shows the discriminative ability indicated by the detection index in the 1h probe test in the Novel Object Recognition, in Sham and SNI rats. P value of <0.05 was considered statistically significant. Each dot indicates a single rat. Each column indicates mean ± SEM.
Data were analysed by One-way or Two-way ANOVA followed by Tukey's multiple comparisons test. *, ** and *** indicate $p < 0.05$, $p < 0.01$ and $p < 0.0001$ vs respective control group. "C" shows the experimental timeline of LTP recordings and "D" represents the schematic diagram of in vivo recordings of long-term potentiation in LEC-DG pathway showing the position of the stimulating (lateral entorhinal cortex, LEC) and recording (dentate gyrus, DG) electrodes and the theta burst stimulation protocol (TBS) to evoke LTP in DG, consisted of 6 trains, 6 bursts, 6 pulses at 400 Hz, interburst interval: 200 ms, intertrain interval: 20 s "E" shows representative traces of a single evoked field excitatory postsynaptic potentials (fEPSP) recorded in DG before and after TBS protocol (black arrow). "F" shows the time-dependent changes in the fEPSP amplitude after TBS protocol application. Data plotted as % amplitude from baseline (pre-TBS). Data points represent averaged slope (mean ± SEM) after TBS induction, normalized with respect to baseline values (pre-TBS). "G" shows a bar histogram of amplitude data averaged 30–60 min after TBS and normalized respect to the baseline (mean ± SEM). "H" shows data points representing averaged slope (mean ± SEM) after TBS induction, normalized with respect to baseline values (pre-TBS). "I" shows a bar histogram of slope data averaged 30–60 min after TBS and normalized respect to the baseline (mean ± SEM). * and ** indicate $p < 0.05$ and $p < 0.01$, respectively, vs pre-TBS (-30-0 min).

another 7 consecutive 30-min dialysate samples were collected to record the post-injection effects of the drug. Upon completion of the experiments, rats underwent transcardial perfusion with saline (0.9%) followed by paraformaldehyde. The brains were then extracted, fixed in a 10% formaldehyde solution for 2 days, and sectioned into 40-mm thick slices. Probe locations were verified under a light microscope.

Dialysate samples were subjected to analysis via high-performance liquid chromatography (HPLC). The HPLC system comprised a Varian ternary pump (mod. 9010), a C18 reverse-phase column (Supelco Discovery, 5 μm particle size, L × I.D. 25 cm × 4.6 mm), and a Varian fluorimetric detector. Prior to injection, dialysates were derivatized with opthaldialdehyde-N-acetylcysteine (OPA-NAC solution: 10 μL of dialysate, 5 μL of OPA-NAC, and 10 μL of 10% borate buffer) and manually injected using a microsyringe (Hamilton 702 RN). Amino acid conjugates were separated using a gradient separation method, with the mobile phase consisting of two components: (1) 0.2 M sodium phosphate buffer and 0.1 M citric acid (pH 5.8), and (2) 90% acetonitrile and 10% distilled water. The gradient composition was determined using Gilson gradient management software installed on an Apple microcomputer. Data were collected using a Dell Corporation PC system 310 interfaced to the detector through a Drew data collection unit. The mean dialysate concentration of amino acids in the 6 samples represented the basal release. The neurotransmitter content was expressed as the mean ± S.E. M. in pmol/10 μL of dialysate(Ferrara et al., 2019).

2.7. Endocannabinoids levels measurements

Samples (~50 μl) were sonicated and extracted with chloroform/methanol (2:1, vol/vol) containing internal standards for AEA, 2AG, PEA and OEA ($[^2H]_8$ AEA 5 pmol; $[^2H]_5$ 2AG, $[^2H]_4$ PEA, $[^2H]_2$ OEA 50 pmol each). The lipid-containing organic phase was dried down, weighed, and dissolved in 100 μl of methanol for eCB and related molecules a quantification by LC-APCI-MS (LCMS-2020, Shimadzu) as previously reported (Ferrara et al., 2019; Piscitelli et al., 2020; Zamberletti et al., 2017).

2.8. Dynorphin enzyme-linked immunosorbent assay (ELISA)

Dynorphin peptide levels were measured in sham and SNI rat's ventral hippocampus fresh tissue (N = 8–10/group) collected at the end of in vivo analysis, by using Rat Dyn ELISA Kit (CSB-E13294r, Cusabio), according to the manufacturer's instructions. The obtained absorbance values were initially calculated as pg/mL, using a standard curve that was assayed in parallel to the test samples, and then converted into pg/μg of protein (Lorente et al., 2024).

2.9. Immunofluorescence analysis

2.9.1. Brain perfusion and tissue processing

Animals were anesthetized with urethane (1.5 g/kg) administered intraperitoneally (i.p.). Afterwards, animals were perfused transcardially with physiological saline and subsequently with 4% paraformaldehyde, pH 7.4. Brains were removed, post-fixed for 3 h and after cryoprotected with 30% sucrose in PB. Rat brains were sectioned coronally with Leica CM3050S freezing cryostat into 10 μm-thick. The sections were collected in three alternate series and maintained frozen until being processed for immunofluorescence.

2.9.2. Immunofluorescence-labelling

Brain sections of rat hippocampus were treated with PB-Triton 0.3% (PB-T) for 1 h at room temperature (RT) in a humidified chamber, followed by overnight incubation in a mixture of primary antibodies goat anti-KOR1 (1:100; code no. SAB2501442; Sigma-Aldrich, USA),rabbit anti-VGLUT1 (1:500; code no. 135303; Synaptic Systems, Germany) or guinea pig anti-VGLUT1 (1:200; code no. 135 304; Synaptic Systems, Germany), rabbit anti-VGAT (1:500; code no. 131003; Synaptic Systems, Germany) or guinea pig anti-VGAT (1:200, code no. 131 004; Synaptic Systems, Germany), rabbit anti-CB1 (1:500; code no. ab23703; Abcam, Canada). Immunoreactivity was detected using a specific and appropriate mixture of secondary anti-IgGs antibodies (Invitrogen, ThermoFisher Scientific, France) Alexa-594 donkey anti-goat (A11058, 1:50), Alexa-488 donkey anti-rabbit (A21206, 1:250), Alexa-594 goat anti-rabbit (A11010,1:250), Alexa-488 goat anti-guinea pig (A11073,1:100), Alexa-594 donkey anti-rabbit (A21207,1:250) and Alexa-488 donkey anti-goat (A11055, 1:250). The sections were then counterstained with DAPI (4',6-diamidino-2-phenylindole) (Sigma-Aldrich, USA) and cover slipped with aqueous mounting medium Aquatex (Merck, Darmstadt, Germany). Controls of specificity of immunolabeling in multiple fluorescence were performed by omission of primary and/or secondary antibodies or by preadsorbtion of primary antibodies with the respective blocking peptides. The immunostained sections were observed with a confocal microscopy Nikon Eclipse Ti2 (Nikon, Japan) equipped with an x-y-z motorized stage, a digital camera DS-Qi2. Digital images were acquired using the × 10− × 20 objectives. The brain regions of interest were identified by referencing the Paxinos & Watson rat brain atlas.

2.9.3. Quantification

Quantitative assessment of immunolabeling was conducted by collapsing serial Z plane images into a two-dimensional image (n ≤ 30 planes with an increment of 0.5 μm). The percentage of KOR1, VGLUT, VGAT and CB1 immunolabeled areas, was quantified with respect to the anterior−posterior extent of the DG area in a series of 10 μm coronal sections spaced 30 μm apart (1:3 as the frequency of section sampling for immunohistochemistry) collected starting from Bregma −3.30 mm up to Bregma −4.30 mm, through 1 mm^3 rostrocaudal extension from the hilus bifurcation. To evaluate multiple markers co-localization a Manders' Colocalization Coefficients (MCC) analysis was performed using the ImageJ J ACoP plug-in, describing the contribution from two selected channels to the pixels of interest by providing measures of the fraction of total probe fluorescence that colocalizes with the fluorescence of a second probe (Dunn et al., 2011). Data collection was randomized across all experiments, and experimenters remained blinded by imaging and data analysis.

2.10. Study design

A total number of 78 animals was analysed and they were randomly divided in the following experimental groups.

A. **Sham/Veh** that received intraperitoneal injection of vehicle for 7 days starting from 7 days post-surgery
B. **Sham/CBD** that received intraperitoneal injection of CBD (5 mg/kg) for 7 days starting from 7 days post-surgery
C. **SNI/Veh** that received intraperitoneal injection of vehicle for 7 days starting from 7 days post-SNI
D. **SNI/nor-BNI** that received a single subcutaneous injection of Nor-Binaltorphimine (10 mg/kg) on the day of the experiment
E. **SNI/CBD** that received intraperitoneal injection of CBD (5 mg/kg) for 7 days starting from 7 days post-SNI
F. **SNI/CBD + nor-BNI** that received a single subcutaneous injection of Nor-Binaltorphimine (10 mg/kg) 7 days after CBD, on the day of the experiment

In vivo evaluations (mechanical allodynia, novel object recognition test, LTP and microdialysis) were performed fourteen days post-surgery, in both sham-operated and SNI rats. At the end of in vivo observation, animals were euthanized, and tissues were collected for biochemical and immunofluorescence analysis.

2.11. Drugs

Cannabidiol (CBD) (Sigma-Aldrich), Nor-Binaltorphimine (nor-BNI) (cat. No. N1771) and the vehicle solution (DMSO, water 1:9) (cat. No. D2650) were purchased from Sigma-Aldrich. CBD (5 mg/kg) and the vehicle were administered intraperitoneally for 7 days starting from 7 days after SNI induction. Conversely, nor-BNI (10 mg/kg) was administered subcutaneously, 1 h prior to conducting in vivo evaluations. CBD and nor-BNI doses and the treatment schedule were selected based on previous evidence on their efficacy in preclinical model of neuropathic pain (De Gregorio et al., 2019; Mei Xu et al., 2004).

2.12. Statistical analysis

Statistical analysis was performed by using GraphPad Prism 8 (GraphPad Software, La Jolla, CA, USA). Normality was evaluated using Shapiro-Wilk's test. Behavioural datasets with normal distribution were analysed for significance using a two-way ANOVA for repeated measures followed by Tukey's multiple comparisons test post hoc test for comparisons between groups or one-way ANOVA followed by Tukey's multiple comparison post hoc test for multiple comparisons within groups.

Biochemical datasets were statistically analysed using one-way ANOVA followed by Tukey's multiple comparison test.

For immunofluorescence statistical analyses, normality of data distribution was assessed using the Kolmogorov–Smirnov or Shapiro–Wilk test, and equality of variance was confirmed using the F-test. Data from multiple groups were analysed by one-way ANOVA and two-way ANOVA (Brown-Forsythe and Welch ANOVA test), followed by Dunnett's T3 post hoc tests.

A probability level of $p < 0.05$ was statistically significant. Results are presented as mean ± standard error of the mean (SEM).

3. Results

3.1. CBD alone or in combination with nor-BNI reverted mechanical allodynia in SNI rats

The mechanical withdrawal threshold to the innocuous stimulus (a steel rod applied with increasing force, reaching 0–100 g over 10 s) was measured (85.00 ± 7.319 g) in sham rats injected with vehicle (Fig. 1A). One-way ANOVA for repeated measures followed by Tukey's multiple comparisons test revealed significant differences among treatments' groups ($F_{(5,35)} = 5.015$, $P = 0.0014$). Administration of CBD did not elicit any significant alteration in the mechanical response threshold in sham rats (71.118 ± 11.937 g) (Fig. 1A). The SNI of sciatic nerve induced a substantial reduction in the mechanical withdrawal threshold in the ipsilateral paw (23.500 ± 5.763 g; $P = 0.0013$) compared to sham rats receiving vehicle. Conversely, administration of CBD in SNI rats resulted in a significant increase in the mechanical withdrawal threshold (70.750 ± 9.479 g; $P = 0.0211$) compared to SNI rats treated with vehicle alone (Fig. 1A). Moreover, of the acute nor-BNI injection in repeatedly CBD-treated SNI rats did not alter anti-allodynic effect of CBD (76.500 ± 12.052 g; $P = 0.0072$) (Fig. 1A).

3.2. CBD or nor-BNI ameliorated the short-term recognition memory in SNI rats. On the contrary, this effect was reduced when CBD-treated rats were pre-treated with nor-BNI

To assess discriminative memory, considered one of the main comorbidities associated with neuropathic pain, we carried out the Novel Object Recognition Test. The total exploration time during the familiarization session was not significantly different between the SNI model and the sham group (1.309 ± 0.058 vs. 1.214 ± 0.147; $P = 0.9965$) (not shown). However, it was observed that the SNI model caused a significant reduction in discriminative abilities in the SNI/Veh-treated rats compared to the sham group (−0.077 ± 0.032 vs. 0.211 ± 0.030; $P = 0.0057$) (Fig. 1B). One-way ANOVA followed by Tukey's multiple comparisons test revealed significant differences among treatment groups ($F_{(5,35)} = 12.20$; $P < 0.0001$). The treatment with CBD led to an improvement in cognitive performance in the SNI/CBD group compared to the SNI/Veh-treated group (0.306 ± 0.068 vs. −0.077 ± 0.032; $P = 0.0001$). Similarly, the administration of nor-BNI improved the discriminative abilities of the SNI/nor-BNI group compared to the SNI/Veh-treated group (0.285 ± 0.077 vs. −0.077 ± 0.032; $P = 0.0003$) (Fig. 1B). However, no significant effect was observed in the sham/CBD-treated group compared to the sham group (0.321 ± 0.059 vs. 0.211 ± 0.030; $P = 0.6796$). Interestingly, the group treated with the combination of CBD and nor-BNI did not show an improvement in cognitive performance compared to the SNI/Veh-treated group (−0.059 ± 0.039 vs. −0.077 ± 0.032; $P = 0.9999$) (Fig. 1B).

3.3. CBD and nor-BNI retrieved the long-term potentiation in LEC-DG pathway and this effect was blocked by nor-BNI in SNI rats

To assess the potential effect of CBD and nor-BNI on synaptic plasticity in SNI rats, LTP recordings were performed in LEC-DG pathway in hippocampus, 14 days post-SNI (7 days post-treatment), as shown in Fig. 1C and D. As previously found in SNI mice (4), the TBS application in the LEC failed to induce potentiation of post-synaptic responses in DG in SNI (Fig. 1E–I) rats treated with vehicle, 14 days post-injury. Indeed, no changes of the fEPSPs amplitude (30–60 min: 102.23 ± 4.60 *vs* 0–15 min: 100.53 ± 3.06 %) ($p = 0.99$) (Fig. 1E and F and G) and slope (30–60 min: 105.03 ± 4.81 *vs* 0–15 min: 99.15 ± 2.93 %) (Fig. 1E–H and I) ($p = 0.96$) were observed after TBS application differently from sham rats that showed a significant increase in both amplitude (30–60 min: 185.34 ± 3.9 *vs* 0–15 min: 101.01 ± 0.2 %) ($p < 0.001$) and slope (30–60 min: 141.56 ± 3.69 *vs* 0–15 min: 99.66 ± 0.76 %) ($p = 0.0144$) that kept stable until the end of the experiment (Fig. 1E–I). A similar effect was observed in sham rats that received subcutaneously treatment with CBD for 7 days (5 mg/kg), amplitude (30–60 min: 171.22 ± 5405% *vs* 0–15 min: 100.348 ± 0.27%) ($p = 0.0011$) and slope (30–60 min: 199.59 ± 16.97% *vs* 0–15 min: 100.378 ± 0.45%) ($p < 0.001$) (Fig. 1E–I)

Two-way ANOVA followed by Tukey's post-hoc test revealed significant differences in the amplitude between treatments ($F_{(5, 48)} = 7.864$, $P < 0,0001$), time ($F_{(1, 48)} = 93.58$, $P < 0,0001$) and treatment × time interaction ($F_{(5, 48)} = 8.454$, $P < 0.0001$) of EPSPs was observed. The same result was obtained for differences in the slope between treatments ($F_{(5, 48)} = 24.52$ $P < 0.0001$), time ($F_{(1, 48)} = 180.7$, $P < 0.0001$) and treatment × time interaction ($F_{(5, 48)} = 23.78$, $P < 0.0001$) of EPSPs.

Intriguingly the repeated treatment with CBD significantly reversed the LTP impairment as compared to vehicle-treated SNI rats, 14 days post-injury (Fig. 1E–I). In particular, fEPSPs amplitude and slope from 30 to 60 min post-TBS for SNI rats treated with CBD were: 206.13 ± 32.02 % ($p = 0.0013$) and 178.12 ± 17.22 % ($p = 0.0018$). The single injection with the nor-BNI instead showed a trend in improving the LTP functioning on both amplitude (179.66 ± 10.54%; $p = 0.0002$) and slope (229.59 ± 3.01%; $p < 0.0001$) (Fig. 1E–I).

Surprisingly, the co-treatment with CBD and nor-BNI in SNI rat, abolished the protective effect of single compounds on synaptic plasticity. Indeed, TBS application was not able to induce potentiation of fEPSPs in SNI rats (Fig. 1E). Specifically, the amplitude was 109.49 ± 9.83% from 30 to 60 min compared to 100.24 ± 3.40% from 0 to 15 min ($p > 0.99$) (Fig. 1E and F and G), and the slope were 97.48 ± 5.90% at 30–60 min compared to 98.91 ± 3.23% at 0–15 min ($p > 0.99$) (Fig. 1E–H and I).

3.4. Effect of CBD and nor-BNI on glutamate and GABA release in the DG of sham and SNI rats

Microdialysis coupled with HPLC revealed that extracellular L-Glu levels in the DG of the Sham/CBD group before injection of nor-BNI were significantly higher compared to the Sham/Veh group (13.80 ± 1.03 vs 7.70 ± 1.04 pmol/10 μl; F (7,19) = 4, P = 0.0074), and also compared to the SNI/CBD group before drug injection (13.80 ± 1.03 vs 7.19 ± 3.67 pmol/10 μl; $F_{(7,19)}$ = 4, P = 0.0074), suggesting saturation of glutamatergic signaling. However, no change was observed in L-Glu levels following nor-BNI injection into the DG of the animals (Fig. 2A).

The extracellular GABA levels in the DG of the SNI/CBD group before injection of nor-BNI were significantly lower compared to both the SNI/Veh group (10.20 ± 1.01 vs. 20.37 ± 3.17 pmol/10 μl; $F_{(7,24)}$ = 4, P < 0.0001) and the Sham/CBD group (10.20 ± 1.01 vs. 15.046 ± 1.57 pmol/10 μl; $F_{(7,24)}$ = 4, P < 0.0001) (Fig. 2B). Moreover, a significant increase was observed in GABA levels in the sham/veh group after nor-BNI injection compared to basal levels (18.65 ± 1.85 vs. 27.44 ± 4.63 pmol/10 μl; F ($_{7,24}$) = 4, P < 0.0001), indicating a potential modulation of GABAergic signaling pathways (Fig. 2B). Similarly, an increase in GABA levels was also observed in the SNI/Veh group (20.37 ± 3.17 vs. 26.75 ± 2.07 pmol/10 μl; F ($_{7,\ 24}$) = 4, P < 0.0001) and the SNI/CBD group (10.20 ± 1.01 vs. 19.93 ± 7.77 pmol/10 μl; F ($_{7,24}$) = 4, P < 0.0001) following nor-BNI injection, suggesting a potential disruption in GABAergic signaling following nerve injury (Fig. 2B). However, no significant change in GABA levels was observed in the SNI/Veh group after nor-BNI injection compared to basal levels, suggesting a lack of effect on GABAergic signaling pathways following administration of nor-BNI (Fig. 2B). These findings highlight the complex interplay between cannabinoid treatment, nerve injury, and GABAergic signaling as well as L-Glu level within the dentate gyrus region of the rat brain.

3.5. CBD and nor-BNI, alone or in combination, mitigate the upregulation of VGLUT1 and VGAT in the DG of SNI rats

Based on the amino acids levels changes, we performed immunohistochemical analysis the showed increased staining of VGLUT1 and VGAT mostly found in granule cells layer and highly in the molecular layer of DG of SNI rats. As observed by analysis of immunolabeled VGLUT1-or VGAT positive area in DG we found a reduction in the expression of the vesicular transporter for either excitatory and inhibitory neurotransmitter release in SNI rats treated with CBD and nor-BNI, each alone, or in combination (Fig. 2C and D). As assessed by one-way ANOVA, analysis for VGLUT1 fluorescence ($F_{(4,\ 40)}$ = 87.62; P < 0.0001), Sidak's multiple comparison test revealed that Sham-Veh (2.758 ± 0.1627) shows a significant difference (P < 0.0001) compared to SNI/Veh (5.795 ± 0.1831). SNI-Veh shows a significant difference (P < 0.0001) compared to SNI/CBD (2.071 ± 0.1355). SNI-Veh shows a significant difference (P < 0.0001) compared to SNI/nor-BNI (2.591 ± 0.1978). SNI-Veh shows a significant difference (P < 0.0001) compared to SNI/nor-BNI + CBD (4.436 ± 0.1455) (Fig. 2C). Moreover, one-way ANOVA ($F_{(4,\ 40)}$ = 87.62; P < 0.0001) and Sidak/s post hoc test indicates that Sham/Veh (2.421 ± 0.1414) shows a significant difference (P < 0.0001) compared to SNI/Veh (4.025 ± 0.1702). SNI/Veh shows a significant difference (P < 0.0001) compared to SNI/CBD (1.903 ± 0.1230). SNI/Veh shows a significant difference (P < 0.0001) compared to SNI/nor-BNI (1.696 ± 0.1235). SNI-Veh shows a significant difference (P < 0.0001) compared to SNI/nor-BNI + CBD (0.9344 ± 0.08831. SNI/CBD shows a significant difference (P < 0.0001) compared to SNI/nor-BNI + CBD (Fig. 2D) as revealed by one-way ANOVA test with Sidak's multiple comparisons post-hoc test.

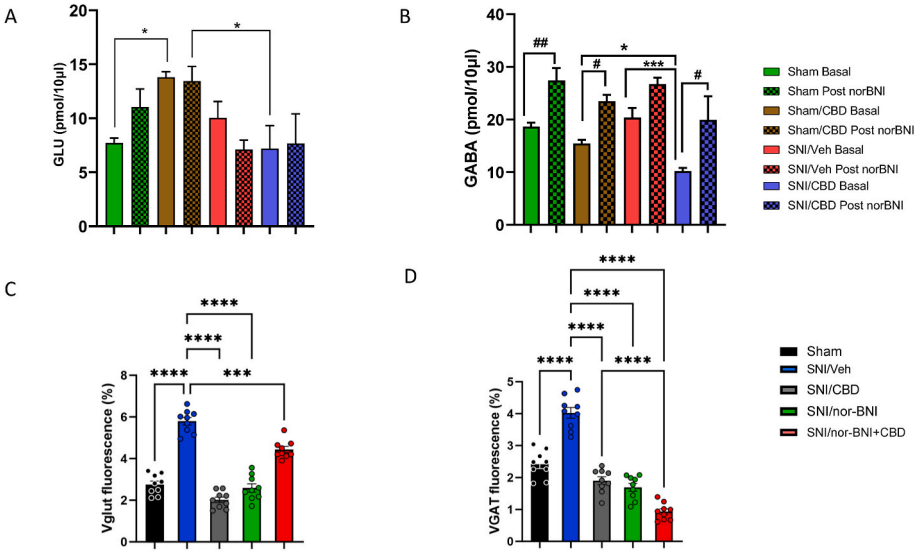

Fig. 2. Effect of CBD and nor-BNI on glutamate and GABA release and VGLUT1 and VGAT expression. "A and B" show L-Glu and GABA extracellular levels in DG, respectively. All data are expressed as the mean average ± SEM of 5 animals per group. P < 0.05 was considered statistically significant. # shows the difference between the basal level and post-nor-BNI injection level of the neurotransmitters, and * indicates the difference between the basal level of the neurotransmitters between the groups. "C" shows the quantitative analysis of VGLUT1 immunolabeled fluorescent micrographs of rat DG. Rat brains were evaluated in absence or presence of spared nerve injury (SNI) and treated respectively with Cannabidiol (CBD) and Nor-binaltorphimine (nor-BNI), alone or in presence of CBD (nor-BNI + CBD). Data are presented as means ± SEM for the percentage of VGLUT1 immunoreactive area in DG area (from Bregma −3.30 to −4.30 mm) from n = 3 rats per experimental condition. "D" shows a quantitative analysis of VGAT immunolabeled fluorescent micrographs of rat DG. Rat brains were evaluated in absence or presence of spared nerve injury (SNI) and treated respectively with Cannabidiol (CBD) and nor-binaltorphimine (nor-BNI), alone or in presence of CBD (nor-BNI + CBD). Data are presented as means ± SEM for the percentage of VGLUT1 immunoreactive area in DG area (from Bregma −3.30 to −4.30 mm) from n = 3 rats per experimental condition. Statistical analyses were conducted using a Shapiro-Wilk test and/or Kolmogorov-Smirnov test to assess the Normal or Lognormal data distribution and then analysed with Brown-Forsythe and Welch's ANOVA test with Dunnett's T3 multiple comparisons post-hoc test. (For interpretation of the references to colour in this figure legend, the reader is referred to the Web version of this article.)

3.6. CBD reduces SNI-induced dynorphin peptide and KOR1 overexpression in the ventral hippocampus

One-way ANOVA indicated a statistically significant difference in dynorphin peptide levels among treatment's group ($F_{(4,39)} = 10.13$; $P < 0.0001$). Tukey's multiple comparisons test showed that dynorphin peptide levels were significantly increased in the ventral hippocampus of SNI/vehicle rats in respect to Sham animals (0.89 ± 0.09 vs 0.47 ± 0.02; $P < 0.0001$). Chronic administration of CBD caused a significant reduction of dynorphin levels in SNI rats (0.66 ± 0.05 vs 0.89 ± 0.09; $P = 0.047$). The kappa antagonist nor-BNI, either administered alone or after CBD prolonged treatment, reduced dynorphin levels in SNI rats (0.56 ± 0.06 vs 0.89 ± 0.09; $P = 0.0015$, alone; 0.46 ± 0.03 vs 0.89 ± 0.09; $P < 0.0001$, in combination) (Fig. 3 A).

Immunohistochemical analysis revealed a significant SNI-mediated induction of KOR1 reactivity, mainly localized at the granular cell layer of DG. KOR1 immunoreactivity, analysed by One-way ANOVA test ($F_{(4, 40)} = 63.26$; $P < 0.0001$), was lowered by CBD administration in SNI rats, and this effect was blocked by nor-BNI in SNI rats (Fig. 3 B and E). Dunnet's T3 multiple comparison test reported that Sham/Veh (2.212 ± 0.097) shows a significant difference ($F = 10$, $P < 0.0001$) compared to SNI/Veh (6.018 ± 0.2719). SNI-Veh shows a significant difference ($P < 0.0001$) compared to SNI/CBD (1.758 ± 0.1305). SNI/CBD shows a significant difference (, $P < 0.0001$) compared to SNI/nor-BNI + CBD (4.763 ± 0.2137). KOR1/VGLUT1 expression was highly colocalized at granular layer of DG in SNI/Vehicle and SNI/nor-BNI and this colocalization was reduced by CBD or CBD/nor-BNI injection in rats as indicated by One-way ANOVA test ($F_{(4, 40)} = 21.9$; $P < 0.0001$) (Fig. 3 C and E). Indeed, Sidak's test revealed that, SNI/Veh (0.1971 ± 0.01411) shows a significant difference ($P < 0.0001$) compared to SNI/CBD (0.06167 ± 0.008526). SNI/CBD shows a significant difference ($P = 0.0306$) compared to SNI/nor-BNI + CBD (0.1231 ± 0.008978). Similarly, KOR1/VGAT immunoreactivity (One-way ANOVA test, $F_{(4, 40)} = 40.64$; $P < 0.0001$) in DG was highly colocalized in SNI/Vehicle but CBD/nor-BNI co-treatment in SNI rats was less efficient to reduce the overexpression then CBD or nor-BNI alone (Fig. 3D and E) from Sham/Vehicle- or SNI/vehicle-injected rats, and from SNI/CBD- or SNI/nor-BNI- or SNI/CBD/nor-BNI-treated rats. KOR immunoreactivity in the granule cells layer continued to be very high except in VGLUT1 nerve terminals where it was reduced by nor-BNI (Fig. 3 C and E). Finally, Sham/Veh (0.05489 ± 0.01007) shows a significant difference ($P < 0.0001$) compared to SNI/Veh (0.2130 ± 0.01093). SNI-Veh shows a significant difference ($P < 0.0001$) compared to SNI/CBD (0.1160 ± 0.01067), as revealed by one-way ANOVA test with Dunnett's T3 or Sidak's multiple comparisons post-hoc test.

3.7. Effect of CBD and nor-BNI on endocannabinoids levels and CB1 expression glutamatergic or GABAergic terminals

Extracellular levels of AEA showed no changes in the Sham groups;

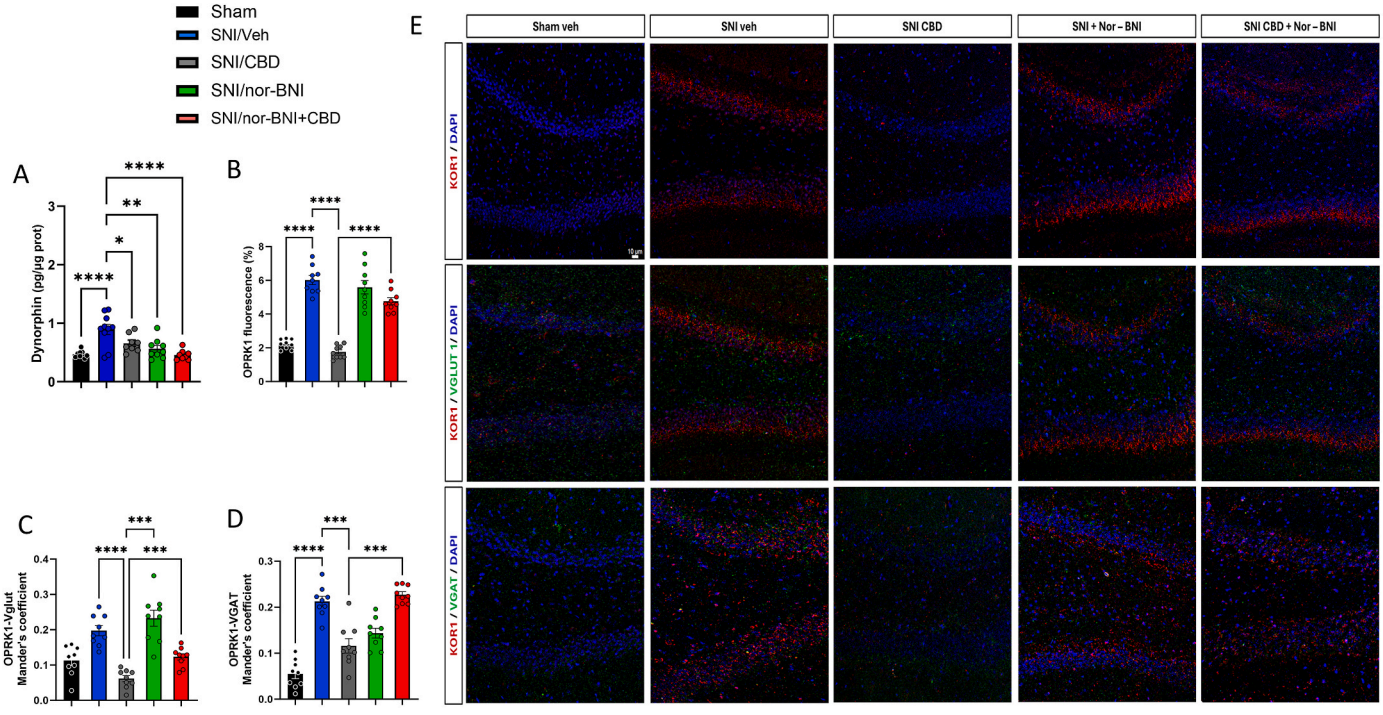

Fig. 3. CBD reduces SNI-induced dynorphin peptide and KOR1 overexpression in the ventral hippocampus "A" shows dynorphin levels measured by ELISA assay in the ventral hippocampus in Sham and SNI rats treated with CBD, nor-BNI or their combination. Data are expressed as means ± SEM of 8–10 animals per group and were analysed by One-way ANOVA followed by Tukey's multiple comparison test. "B" shows the quantitative analysis of OPKR1 immunolabeling in DG of Sham or SNI rats, treated with Cannabidiol (CBD), or nor-binaltorphimine (nor-BNI) or both (nor-BNI + CBD). "C" shows the Mander colocalization coefficient analysis of OPKR1/VGLUT immunolabeled fluorescent micrographs of immunolabeled fluorescent micrographs of Sham or SNI rats, treated with Cannabidiol (CBD), or nor-binaltorphimine (nor-BNI) or both (CBD/nor-BNI). Data are presented as means ± SEM for the Mander's coefficient the percentage of VGLUT1 immunoreactive area in DG area (from Bregma −3.30 to −4.30 mm) from n = 3 rats per experimental condition. "E" shows the Mander colocalization coefficient analysis of OPKR1/VGAT immunolabeled fluorescent micrographs of immunolabeled fluorescent micrographs of Sham or SNI rats, treated with Cannabidiol (CBD), or nor-binaltorphimine (nor-BNI) or both (nor-BNI + CBD). "E" shows the representative micrographs of KOR1/DAPI or KOR1/VGLUT1/DAPI, and KOR1/VGAT/DAPI immunolabeling of the dentate gyrus (DG) from the hippocampus of Sham/Veh or SNI/Veh-injected rats, and of SNI/CBD- or SNI/nor-BNI- or SNI/nor-BNI + CBD-treated rats. Data are presented as means ± SEM for the Mander's coefficient the percentage of OPKR1/VGAT immunoreactive area in DG area (from Bregma −3.30 to −4.30 mm) from n = 3 rats per experimental condition. Statistical analyses were conducted using a Shapiro-Wilk test and/or Kolmogorov-Smirnov test to assess the Normal or Lognormal data distribution and then analysed with Brown-Forsythe and Welch's ANOVA test with Dunnett's T3 multiple comparisons post-hoc test. (For interpretation of the references to colour in this figure legend, the reader is referred to the Web version of this article.)

however, a significant decrease was observed following SNI/CBD after nor-BNI treatment compared to the SNI/CBD basal levels ($P < 0.05$, Fig. 4A). In contrast, 2-AG levels exhibited significant alterations in both the Sham and SNI groups. Notably, the extracellular 2-AG concentration was lower in the Sham/CBD basal and SNI/veh groups compared to the Sham/basal group (Fig. 4B). Furthermore, nor-BNI treatment led to an increase in extracellular 2-AG levels in the DG, in both SNI/Veh and SNI/CBD groups, compared to their respective control groups (Fig. 4B, $P < 0.0001$ for SNI/Veh basal and $P < 0.01$ for SNI/CBD basal). Finally, CB1 receptors were increased by neuropathy at the granular layer and reduced by CBD and nor-BNI, alone or in combination as statistically described with one way ANOVA ($F_{(4,\ 40)} = 253.8$; $P < 0.0001$). In particular, in Sidak's multiple comparison, Sham/Veh (4.928 ± 0.1694) shows a significant difference ($P < 0.0001$) compared to SNI/Veh (9.670 ± 0.1267). SNI/Veh shows a significant difference ($P < 0.0001$) compared to SNI/CBD (3.282 ± 0.09537). SNI/Veh shows a significant difference ($P < 0.0001$) compared to SNI/nor-BNI + CBD (1.348 ± 0.07234). SNI/CBD shows a significant difference ($P < 0.0001$) compared to SNI/nor-BNI + CBD (Fig. 4D)

Intriguingly, CBD promotes CB1 expression at both excitatory (VGLUT1) (Fig. 4 C and E) and inhibitory (VGAT) (Fig. 4 C and F) inputs. For CB1/VGLUT1 colocalization were analysed through one way ANOVA ($F_{(4,\ 40)} = 96.32$; $P < 0.0001$) Sham/Veh (0.03744 ± 0.009812) shows a significant difference ($P < 0.0001$) compared to SNI/Veh (0.1658 ± 0.0138). SNI/nor-BNI (0.2773 ± 0.007835) shows a significant difference ($P = 0.0217$) compared to SNI/nor-BNI + CBD (0.2257 ± 0.006737). SNI/Veh shows a significant difference ($P < 0.0001$) compared to SNI/nor-BNI. SNI/Veh shows a significant difference ($P = 0.0053$) compared to SNI-nor-BNI + CBD (Fig. C and E). For CB1/VGAT colocalization (one way ANOVA, $F_{(4,\ 40)} = 57.53$; $P < 0.0001$), Sham/Veh (0.09278 ± 0.01039) shows a significant difference ($P < 0.0001$) compared to SNI/Veh (0.2678 ± 0.01744), after Sidak's post hoc test. SNI/CBD (0.3461 ± 0.01176) shows a significant difference ($P < 0.0001$) compared to SNI/nor-BNI + CBD (0.1527 ± 0.01456) (Fig. 4D and F).

4. Discussion

We evaluated the protective effects of cannabidiol (CBD) on functional, morphologic, and neurochemical changes in the dentate gyrus of the hippocampus (DG) induced by peripheral neuropathy and the role of KOR on the CBD healing effects. The idea of exploring this drug interaction arises from our and others previous observations that CBD, as well potent KOR activity modulator, reduces pathological pain and the associated affective symptoms (Capasso et al., 2008; De Gregorio et al., 2019; Guida et al., 2012; Medeiros et al., 2024; Scarante et al., 2021).

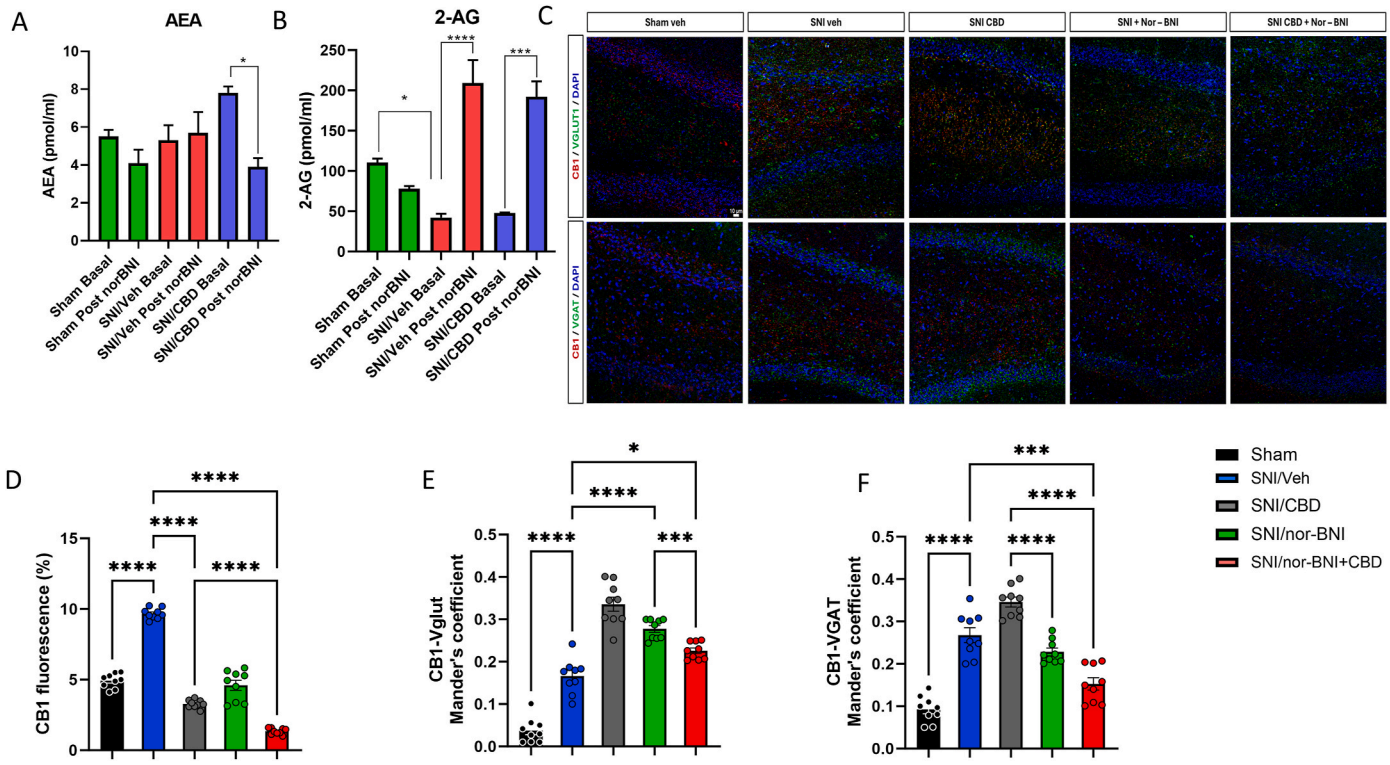

Fig. 4. Effect of CBD and nor-BNI on endocannabinoids levels and CB1 expression glutamatergic or GABAergic terminals "A and B" show the effect of CBD, nor-BNI or CBD + nor-BNI on the levels of the endocannabinoid anandamide (AEA) and 2-arachydonoylglycerol (2-AG) in the DG in sham and SNI rats. "C" shows the representative micrographs of CB1, VGLUT1 and VGAT immunolabeling of the dentate gyrus (DG) from the hippocampus of sham or SNI/vehicle-injected rats, and SNI/CBD or SNI/nor-BNI or SNI/nor-BNI + CBD treated rats. CB1 immunoreactivity is induced in the hilus and granular layer of SNI *vs* sham rats. "D" shows the Mander colocalization coefficient analysis of CB1 immunolabeled fluorescent micrographs of immunolabeled fluorescent micrographs of Sham or SNI rats, treated with Cannabidiol (CBD), or nor-binaltorphimine (nor-BNI) or both (nor-BNI + CBD). Data are presented as means ± SEM for the Mander's coefficient the percentage of CB1 immunoreactive area in DG area (from Bregma −3.30 to −4.30 mm) from n = 3 rats per experimental condition. "E" shows the Mander colocalization coefficient analysis of CB1/VGLUT1 immunolabeled fluorescent micrographs of immunolabeled fluorescent micrographs of Sham or SNI rats, treated with Cannabidiol (CBD), or nor-binaltorphimine (nor-BNI) or both (nor-BNI + CBD). Data are presented as means ± SEM for the Mander's coefficient the percentage of CB1/VGLUT 1 immunoreactive area in DG area (from Bregma −3.30 to −4.30 mm) from n = 3 rats per experimental condition. "F" shows the Mander colocalization coefficient analysis of CB1/VGAT immunolabeled fluorescent micrographs of immunolabeled fluorescent micrographs of Sham or SNI rats, treated with Cannabidiol (CBD), or nor-binaltorphimine (nor-BNI) or both (nor-BNI + CBD). Data are presented as means ± SEM for the Mander's coefficient on DG area (from Bregma −3.30 to −4.30 mm) from n = 3 rats per experimental condition. Statistical analyses were conducted using a Shapiro-Wilk test and/or Kolmogorov-Smirnov test to assess the Normal or Lognormal data distribution and then analysed with Brown-Forsythe and Welch's ANOVA test with Dunnett's T3 multiple comparisons post-hoc test. (For interpretation of the references to colour in this figure legend, the reader is referred to the Web version of this article.)

Given that the interaction between cannabinoid and the opioid systems has emerged (Abrams et al., 2011; Navarro et al., 2001) and considering that CBD has been authorized for the treatment of Lennox-Gastaut epilepsy and Dravet syndrome (Nguyen et al., 2023), we investigated the interactions that CBD might have with opioid receptors (Abrams et al., 2011; Manzanares et al., 1999; Mason et al., 1999; Navarro et al., 2001; Welch, 2009). We confirmed the antiallodynic (Fig. 1A) and anxiolytic (Supplementary Fig. 1) effects of the CBD treatment in a rat model of neuropathic pain (De Gregorio et al., 2019). Interestingly, our data also showed the CBD ability to ameliorate aversive behavior (Supplementary Fig. 1) and memory impairment (Fig. 1B) caused by neuropathic pain condition. This latter behavioral effect was supported by the observed recovery of LTP at the level of the DG of the hippocampus. However, the unexpected finding was that acute KOR inhibition induced two opposite effects in neuropathic rats, depending on whether the animals were pretreated with CBD or not. The KOR antagonist nor-BNI recovered working memory and related synaptic plasticity in the DG of rats not pretreated with CBD. In contrast, nor-BNI reinstated some neuropathic syndrome signs in rats treated with CBD in which this latter alone was effective, thus indicating a subtractive drug-drug interaction. Furthermore, KOR blockade proved ineffective in reducing mechanical allodynia and anxiety-like behaviour. This is not entirely surprising as it is the activation and not the blockade of the KOR that reduces allodynia in neuropathic syndromes (Wang Y.-J. et al., 2016; Xu M. et al., 2004). Indeed, in some instances, the KOR activation by endogenous dynorphin (Wang Y-J. et al., 2016) or salvinorin A (McCurdy CR. et al., 2006) exhibited anti-nociceptive or anxiolytic action after spinal nerve ligation (SNL).

To try to explain these results, we performed further experiments by using in vivo microdialysis to measure glutamate, GABA, anandamide (AEA) and 2-arachidonoyl glycerol (2-AG) levels in DG, in vivo electrophysiology and morphological studies. Moreover. dynorphin peptide in the DG was measured by ELISA.

Unlike a previous study showing change in glutamate (Saffarpour et al., 2017), we did not find changes in DG glutamate or GABA of SNI rats, even during or after LPP tetanization (Jay et al., 1999). The lack of change in extracellular glutamate and GABA levels may fit with the upregulation of synaptic vesicular glutamate or GABA transporters, vGLUT1 and vGAT, respectively, in the DG of SNI rats. Indeed, the lack of mobilization and emptying of the presynaptic vesicles (i.e. their increased staining/accumulation in somatodendritic terminals of the granular cells) could explain the lack of modification in the levels of GABA and glutamate, even if in fact their reduction was expected. Extracellular reduction may have been more the case for GABA where CB1 receptors were overexpressed in vGAT + fibers. The increased CB1 receptor staining could in turn be a compensatory mechanism resulting from a reduction in extracellular levels of 2-AG.

This apparent functional “freezing” of GABA and glutamate extracellular release, together with the reduction in 2-AG, may contribute to the increase in DG dynorphin. Thus, the higher KOR opioid tone disrupted functioning of the granular cells of the DG, as well as of the excitatory terminals originating from the entorhinal cortex (lateral perforant pathway, LPP), ultimately inhibiting hippocampal plasticity and memory (Hollnagel, J.-O. et al., 2019). However, our previous works described increased glutamate in the hippocampus of neuropathic mice (Boccella et al., 2019; Guida et al., 2015). In those works, the glutamatergic hyperactivation caused a “saturation” of normal excitatory transmission with a failure in LTP induction (Boccella et al., 2019).

In the DG, dynorphin is synthesized by granule cells and released from their dendrites. While it mainly has an inhibitory function (Simmons et al., 1995), it can also unexpectedly increase the excitability of granule cells via KOR autoreceptors (Schrader et al., 2011). This excitatory effect could partially explain the elevated basal fEPSP observed in neuropathic rats. KOR agonists can lower the spike threshold in granule cells, increase the number of spikes with a shorter onset than the first spike, broaden the width of the spikes by half, and shorten the interval between spikes. This general increase in excitability with a selective KOR agonist was prevented by nor-BNI. In this study, we hypothesize that the basal increase in fEPSP amplitude in neuropathic rats is related to elevated levels of dynorphin and overexcitability resulting from KOR activation. The post-receptor mechanisms through which these physiological changes are generated (such as the downregulation of K^+ channels as shown by McDermott and Schrader, 2011) are central to these functional changes and remain the subject of further investigation, though they are not the focus of this study. Another key effect of dynorphin is the inhibition of LPP glutamatergic terminals that innervate the radial dendrites or cell bodies of granule cells, mediated through KOR heteroceptors. As a result of these combined effects of increased extracellular dynorphin, the induction of LTP in the LPP-DG pathway was inhibited in SNI rats (Wagner et al., 1993; Salin et al., 1995; Terman et al., 2000).

CBD, through the complex pharmacodynamics, ranging from ion channels to diversity of molecular target and regulation of gene expression or the CB1-mediated THC effects, reduced allodynia and restored hippocampal plasticity and cognitive function in neuropathic rats. CBD restored vGAT+ and vGLUT + staining on terminals surrounding granule cells and reduced extracellular GABA. The increase in GABAergic tone (without changes in endocannabinoids) may be a key factor in the restoration of LTP in the LPP-DG pathway and in the reduction of neuropathic pain symptoms by CBD. There is evidence that an increase in GABA in the DG prevents LTP and memory impairment (Vučković et al., 2018). In addition, potentiation of GABAergic inhibition is currently adopted as therapeutic strategy for neuropathic pain management. It has been shown that CBD is a positive allosteric modulator at all α containing $GABA_A$ receptors but with a higher efficacy for the α2-containing receptor (T. Bakas et al., 2017), partially explaining the CBD-induced antiallodynic effect in neuropathic animals. On the contrary, its increase due to the persistent inhibition of the KOR (i.e. GABAergic disinhibition) would prevent or counteract its maintenance (Wu et al., 2014). We have found that CBD did not affect the GABA level in healthy conditions but decreased it in neuropathic rats treated with CBD. This suggests that a key CBD-induced change in the DG, relevant for its therapeutic effect, may involve the reduction of GABA levels.

It is important to note that its lowest level was observed only after CBD treatment in neuropathic rats and not under other conditions in this study. We can hypothesize that a key mechanism of CBD, alongside many others yet to be explored, may involve the reduction of GABAergic tone for the achievement of the therapeutic effect.

Regarding acute treatment with nor-BNI, we have shown that, although not effective in reducing allodynia, it may prove useful for the treatment of central cognitive impairment in neuropathic pain. Consistently, the tetanization of the LPP in the presence of nor-BNI again induced LTP in neuropathic rats. These results suggest that a low dose of nor-BNI acts on the limbic system and likely less in the spinal cord, where dynorphin is upregulated and supports allodynia (Navratilova E. et al., 2019). While this remains speculative, it is noteworthy that both behavioral and electrophysiological data support this hypothesis, warranting further investigation in future spinal cord studies. To explain a possible signaling pathways underlying the KOR-dynorphin interaction with synaptic plasticity and cognition, we have performed morphological quantification analysis of c-Jun. Our data (Supplementary Fig. 2) confirm previous studies where it is demonstrated that c-Jun is involved in the upregulation of dynorphin in inflammation or chronic pain by activating DYNCRE3, the promoter of the prodynorphin gene (Messersmith DJ et al., 1996; Messersmith DJ et al., 1998). Interestingly, both CBD and nor-BNI can prevent c-Jun activation, and this could also explain the normalization of dynorphin levels observed here with these pharmacological pretreatments. Since nor-BNI prevents c-Jun activation, one could suppose that the same receptor positively modulates the dynorphin level, revealing maybe the positive feedback of the dynorphinergic tone in neuropathic condition. Indeed, dynorphin plays a

crucial role in the maintenance of chronic neuropathic pain (Wang Z et al., 2001). Furthermore, among the mechanisms of action of CBD, we could think that the regulation of c-Jun is a further way of CBD at the intracellular post-receptor signaling level to decrease cellular over-activation. In any case, these data on c-Jun although preliminary, indicate once again the complexity of the action of the drugs studied here and stimulate further studies dedicated to the topic.

In addition, nor-BNI increased extracellular 2-AG level in the DG, possibly due to disinhibition of neural as well as reactive astrocytes or microglia. This is in line with previous data showing an upregulation of DAG lipase in astrocytes, which influences gliotransmission and regulation of neuron-glial crosstalk in rats (Covelo et al., 2021). Astrocyte-derived, but not neuronal-derived, 2-AG has recently been shown to be necessary to promote neurogenesis and plasticity in the DG of mice (Schuele et al., 2022). The coexistence of KOR and CB1 receptors on "activated" astrocytes may justify the high increase in 2-AG after nor-BNI (Hegyi et al., 2018). The autocrine stimulation of the CB1 receptor on the astrocytes allows further release of 2-AG from those cells when the inhibitory counterpart KOR is blocked, thus strengthening the "endocannabinoid tone" of astrocytes (Hegyi et al., 2018). The 2-AG increase would lead, in turn, to a reduction in dynorphin outflow in the DG where we found upregulation of the CB1 receptors staining. Such a CB1 receptor overexpression in neuropathic rats was normalized or even decreased by a single dose of nor-BNI. The CB1 receptor decrease was probably a consequence of its overstimulation by the high extracellular level of 2-AG. This agonist-induced regulation has been

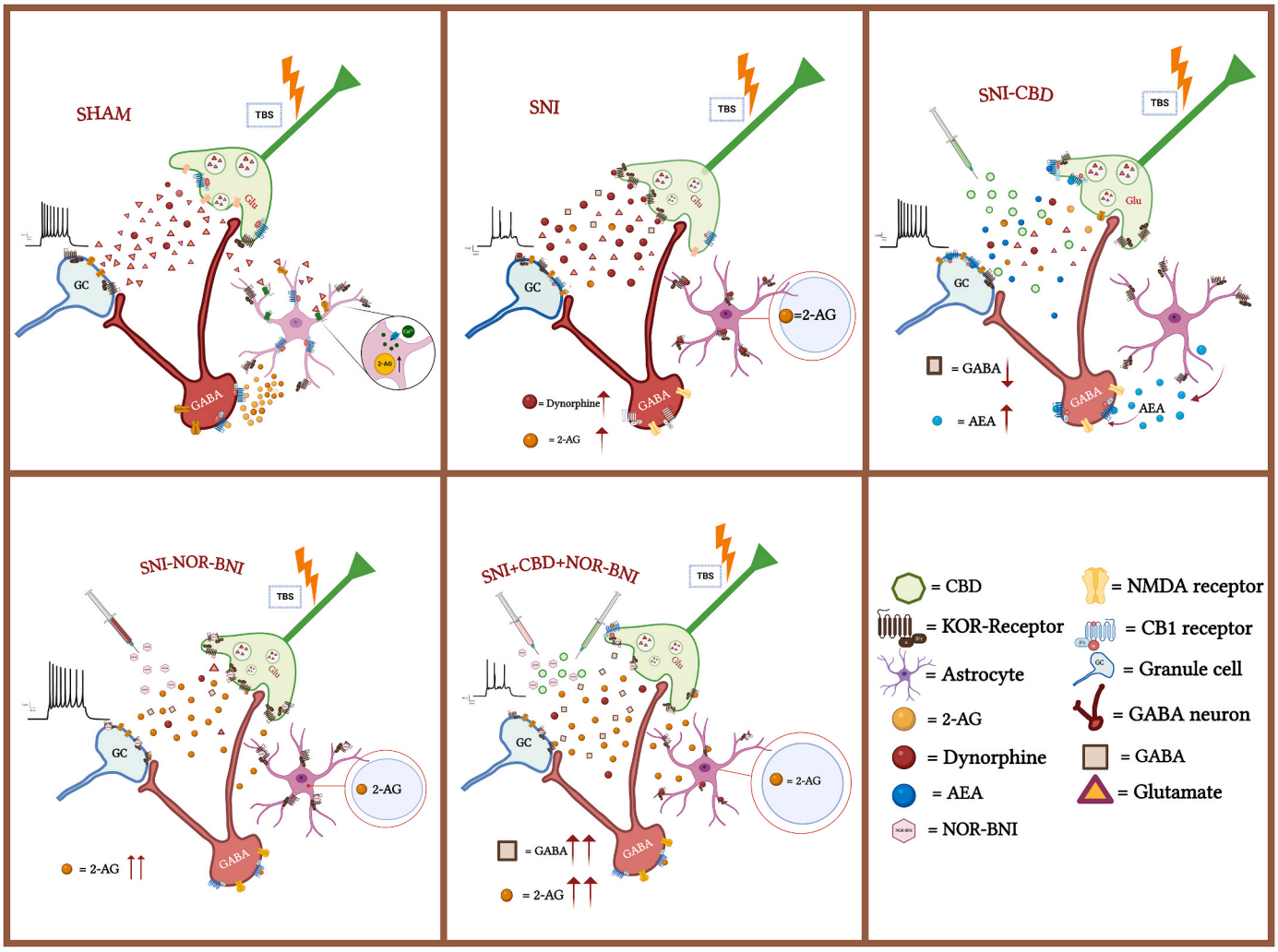

Scheme. A) Physiological condition: under normal physiological conditions, the dentate gyrus presents a typical release of neurotransmitters, including glutamate, GABA and 2-arachidonoylglycerol (2-AG). Long-term potentiation (LTP) is successfully induced after tetanization of the LPP, indicating proper synaptic plasticity and neuronal function. B) Spared nerve injury (SNI) condition: In the SNI condition, there is a notable decrease in the release of 2-AG and GABA, along with an increase in dynorphin secretion. This alteration in neurotransmitter dynamics determines the absence of LTP induction. This reflects reduced synaptic plasticity and potential neuropathic pain states due to upregulation of dynorphinergic tone which in turn inhibits local GABA release. C) SNI condition with CBD administration: cannabidiol (CBD), reduced upregulation of dynorphin and increased anandamide (AEA) level in SNI state. Therefore, the upregulation of AEA exerted its inhibitory effect on GABAergic terminals, the GABA level remained lower compared to control and this contributed to the facilitation of LTP. This neurochemical adjustment restored LTP through a) normalization of CBD-induced dynorphinergic tone, b) a low level of GABA, and c) an increase in AEA which may be critical for the induction of LTP in the LEC-DG pathway. D) SNI condition with NOR-BNI administration: Administration of NOR-BNI, a kappa-opioid receptor (KOR) antagonist, in the SNI condition reduced dynorphin and increased 2-AG levels. Together with KOR inhibition, the massive increase in 2-AG helped preserve LTP induction. This observation indicates a physiological inhibition of KOR on endocannabinoid release and synaptic function. In this condition the GABA level was not changed. E) SNI condition with combined administration of CBD and NOR-BNI: When CBD is administered in combination with NOR-BNI in the SNI condition, there was a marked increase in the release of both 2-AG and GABA. Consistent with the key role of GABA in counteracting the induction of LTP in the hippocampal DG, LTP was not restored. This suggests a complex interaction between the cannabinoid system and GABAergic transmission that is not fully corrected by combined treatment. Indeed, although the very high increase in 2-AG was not in itself effective in those conditions to drive the promotion of LTP, probably due to the CB1 receptor downregulation.

described for the CB1 receptor (Imperatore et al., 2015; Sim-Selley et al., 2006), as well as other GPCRs (Sim-Selley, 2003). Importantly, increased 2-AG, along with elevated AEA, played a crucial role in restoring LTP in the LEC-DG pathway (Boccella et al., 2019; Frazier, 2007; Piomelli, 2003; Wang et al., 2001). Therefore, its reduction in the DG of SNI rats may have contributed to the impaired LTP and memory observed in this study (Kędziora et al., 2023; Murphy N. et al., 2012).

As previously mentioned, acute KOR blockade caused the reappearance of symptoms and signs of neuropathy in CBD-treated rats. Mechanistically we can say that nor-BNI induced a rapid upregulation of KOR, probably as compensation for the slow dissociation kinetics of nor-BNI (Sirohi S. et al., 2016; Bruchas M.R. et al., 2007), and induced a downregulation of CB1 receptors on the same GABAergic terminals. These receptor changes determined a general disinhibition of GABAergic tone in the DG and the reduction of vGAT+ (due to an increase in microvesicular trafficking of GABA and their synaptic depletion) and consequent increase in extracellular levels of GABA. Therefore, we can hypothesize that the blockade of KORs (which were upregulated to compensate for their persistent inhibition by nor-BNI) on vGAT + terminals, along with the downregulation of CB1 receptors (possibly due to elevated 2-AG levels), was a key factor opposing the therapeutic effects of CBD (Scheme 1). While concomitant KOR blockade increased extracellular GABA, further hindering LTP and memory consolidation by CBD (Wu Z. et al., 2014; Schurmans S. et al., 1997; Jo S. et al., 2014), extracellular AEA was also reduced in the DG in these rats. Evidence suggests that AEA is required for LTP in the DG through activation of CB1 receptors (Kędziora et al., 2023; Murphy N. et al., 2012). Although we did not identify the specific cellular source of AEA in this study, AEA may exert inhibitory control over GABAergic terminals. This may also have contributed to the increased GABA and reduced neuroplasticity observed here. In fact, we found that AEA increased when nor-BNI alone reduced neuropathic pain and enhanced neuroplasticity.

5. Conclusions

In conclusion, this study shows that increased dynorphin in the hippocampal DG of neuropathic rats correlates with allodynia and memory deficits. Consistent with other studies, elevated dynorphin in the DG inhibited LTP and was linked to a downregulation of 2-AG and CB1 receptors, highlighting dynorphin's role in discomfort, distress, and pain. This study also confirms the crosstalk between the endocannabinoid and opioid systems; however, several CBD effects are avoided by KOR activity. Both the acute KOR antagonism and 7 days of CBD treatment normalized dynorphin levels and improved affective symptoms, but only CBD had an antiallodynic effect. Notably, acute KOR blockade after CBD treatment caused a recurrence of all the neuropathic pain-related symptoms. Additionally, CBD led to rapid CB1 downregulation and KOR upregulation in the DG, inhibiting LTP and impairing cognition. Collectively, these data suggest that the maintenance of the CBD-restored dynorphinergic tone, likely in combination with other neural adaptive processes, is crucial for the usefulness of a CBD therapeutic treatment.

CRediT authorship contribution statement

Serena Boccella: Writing – review & editing, Writing – original draft, Validation, Methodology, Data curation, Conceptualization. **Antimo Fusco:** Methodology, Data curation. **Federica Ricciardi:** Writing – original draft, Methodology, Data curation. **Andrea Maria Morace:** Methodology, Data curation. **Roozbe Bonsale:** Methodology, Data curation. **Michela Perrone:** Methodology, Data curation. **Ida Marabese:** Methodology, Conceptualization. **Danilo De Gregorio:** Conceptualization. **Carmela Belardo:** Writing – original draft, Data curation. **Luca Posa:** Writing – review & editing, Conceptualization. **Laura Rullo:** Writing – original draft, Methodology, Data curation. **Fabiana Piscitelli:** Writing – review & editing, Methodology, Data curation. **Vincenzo di Marzo:** Writing – review & editing, Conceptualization. **Alessandro Nicois:** Methodology, Data curation. **Brenda Marfella:** Methodology, Data curation. **Luigia Cristino:** Writing – review & editing, Writing – original draft, Methodology, Data curation, Conceptualization. **Livio Luongo:** Conceptualization. **Francesca Guida:** Writing – review & editing, Writing – original draft, Validation, Methodology, Data curation, Conceptualization. **Sanzio Candeletti:** Writing – review & editing, Writing – original draft, Supervision, Conceptualization. **Gabriella Gobbi:** Writing – review & editing, Writing – original draft, Supervision, Resources, Funding acquisition, Conceptualization. **Patrizia Romualdi:** Writing – review & editing, Writing – original draft, Supervision, Resources, Funding acquisition, Conceptualization. **Sabatino Maione:** Writing – review & editing, Writing – original draft, Validation, Supervision, Methodology, Investigation, Data curation, Conceptualization.

Funding

This study was supported by the PSR. Soutien à des initiatives internationales de recherche et Innovation Ministry of Economy and Innovation of Québec, to GG. #NEXTGENERATIONEU (NGEU) provided by the Ministry of University and Research (MUR), and the National Recovery and Resilience Plan (NRRP), project MNESYS (PE0000006)—A multiscale integrated approach to the study of the nervous system in health and disease (DN. 1553 October 11, 2022).

Declaration of competing interest

The authors declare the following financial interests/personal relationships which may be considered as potential competing interests: Serena Boccella reports financial support was provided by This study was supported by the PSR. Soutien à des initiatives internationales de recherche et Innovation Ministry of Economy and Innovation of Québec, to GG. Gabriella Gobbi Danilo De Gregorio reports a relationship with PSR. Soutien à des initiatives internationales de recherche et Innovation Ministry of Economy and Innovation of Québec. that includes: funding grants. Gabriella Gobbi and Danilo De Grgorio has patent #CA3156260A1 pending to Licence. If there are other authors, they declare that they have no known competing financial interests or personal relationships that could have appeared to influence the work reported in this paper.

Appendix A. Supplementary data

Supplementary data to this article can be found online at https://doi.org/10.1016/j.neuropharm.2024.110265.

Data availability

Data will be made available on request.

References

Abrams, D.I., Couey, P., Shade, S.B., Kelly, M.E., Benowitz, N.L., 2011. Cannabinoid-opioid interaction in chronic pain. Clin. Pharmacol. Therapeut. 90 (6), 844–851. https://doi.org/10.1038/clpt.2011.188.

Bakas, T., van Nieuwenhuijzen, P.S., Devenish, S.O., McGregor, I.S., Arnold, J.C., Chebib, M., 2017. The direct actions of cannabidiol and 2-arachidonoyl glycerol at $GABA_A$ receptors. Pharmacol. Res. 119, 358–370. https://doi.org/10.1016/j.phrs.2017.02.022.

Boccella, S., Vacca, V., Errico, F., Marinelli, S., Squillace, M., Guida, F., Di Maio, A., Vitucci, D., Palazzo, E., De Novellis, V., Maione, S., Pavone, F., Usiello, A., 2015. D-aspartate modulates nociceptive-specific neuron activity and pain threshold in inflammatory and neuropathic pain condition in mice. BioMed Res. Int. 2015, 905906. https://doi.org/10.1155/2015/905906.

Boccella, S., Cristiano, C., Romano, R., Iannotta, M., Belardo, C., Farina, A., Guida, F., Piscitelli, F., Palazzo, E., Mazzitelli, M., Imperatore, R., Tunisi, L., de Novellis, V., Cristino, L., Di Marzo, V., Calignano, A., Maione, S., Luongo, L., 2019. Ultra-micronized palmitoylethanolamide rescues the cognitive decline-associated loss of

neural plasticity in the neuropathic mouse entorhinal cortex-dentate gyrus pathway. Neurobiol. Dis. 121, 106–119. https://doi.org/10.1016/j.nbd.2018.09.023.
Capasso, R., Borrelli, F., Cascio, M.G., Aviello, G., Huben, K., Zjawiony, J.K., Marini, P., Romano, B., Di Marzo, V., Capasso, F., Izzo, A.A., 2008. Inhibitory effect of salvinorin A, from Salvia divinorum, on ileitis-induced hypermotility: cross-talk between κ-opioid and cannabinoid CB1 receptors. Br. J. Pharmacol. 155 (5), 681–689. https://doi.org/10.1038/bjp.2008.294.
Caputi, F.F., Rullo, L., Stamatakos, S., Candeletti, S., Romualdi, P., 2019. Modulation of the negative affective dimension of pain: focus on selected neuropeptidergic system contributions. Int. J. Mol. Sci. 20 (16), 4010. https://doi.org/10.3390/ijms20164010.
Cichewicz, D.L., 2004. Synergistic interactions between cannabinoid and opioid analgesics. Life Sci. 74 (11), 1317–1324. https://doi.org/10.1016/j.lfs.2003.09.038.
Covelo, A., Eraso-Pichot, A., Fernández-Moncada, I., Serrat, R., Marsicano, G., 2021. CB1R-dependent regulation of astrocyte physiology and astrocyte-neuron interactions. Neuropharmacology 195, 108678. https://doi.org/10.1016/j.neuropharm.2021.108678.
Cox, M.L., Welch, S.P., 2004. The antinociceptive effect of Delta9-tetrahydrocannabinol in the arthritic rat. Eur. J. Pharmacol. 493 (1), 65–74. https://doi.org/10.1016/j.ejphar.2004.04.022.
De Gregorio, D., McLaughlin, R.J., Posa, L., Ochoa-Sanchez, R., Enns, J., Lopez-Canul, M., Aboud, M., Maione, S., Comai, S., Gobbi, G., 2019. Cannabidiol modulates serotonergic transmission and reverses both allodynia and anxiety-like behavior in a model of neuropathic pain. Pain 160 (1), 136–150. https://doi.org/10.1097/j.pain.0000000000001386.
Decosterd, I., Woolf, C.J., 2000. Spared nerve injury: an animal model of persistent peripheral neuropathic pain. Pain 87 (2), 149–158. https://doi.org/10.1016/S0304-3959(00)00276-1.
Desroches, J., Beaulieu, P., 2010. Opioids and cannabinoids interactions: involvement in pain management. Curr. Drug Targets 11 (4), 462–473. https://doi.org/10.2174/138945010790980303.
Dunn, K.W., Kamocka, M.M., McDonald, J.H., 2011. A practical guide to evaluating colocalization in biological microscopy. Am. J. Physiol. Cell Physiol. 300 (4), C723–C742. https://doi.org/10.1152/ajpcell.00462.2010.
Ferrara, A.L., Piscitelli, F., Petraroli, A., Parente, R., Galdiero, M.R., Varricchi, G., Marone, G., Triggiani, M., Di Marzo, V., Loffredo, S., 2019. Altered metabolism of phospholipases, diacylglycerols, endocannabinoids, and *N* -acylethanolamines in patients with mastocytosis. Journal of Immunology Research 2019, 1–14. https://doi.org/10.1155/2019/5836476.
Guida, F., Luongo, L., Aviello, G., Palazzo, E., De Chiaro, M., Gatta, L., Boccella, S., Marabese, I., Zjawiony, J.K., Capasso, R., Izzo, A.A., De Novellis, V., Maione, S., 2012. Salvinorin A reduces mechanical allodynia and spinal neuronal hyperexcitability induced by peripheral formalin injection. Mol. Pain 8. https://doi.org/10.1186/1744-8069-8-60, 1744-8069-8–60.
Guida, F., Luongo, L., Marmo, F., Romano, R., Iannotta, M., Napolitano, F., Belardo, C., Marabese, I., D'Aniello, A., De Gregorio, D., Rossi, F., Piscitelli, F., Lattanzi, R., De Bartolomeis, A., Usiello, A., Di Marzo, V., De Novellis, V., Maione, S., 2015. Palmitoylethanolamide reduces pain-related behaviors and restores glutamatergic synapses homeostasis in the medial prefrontal cortex of neuropathic mice. Mol. Brain 8 (1), 47. https://doi.org/10.1186/s13041-015-0139-5.
Guida, F., De Gregorio, D., Palazzo, E., Ricciardi, F., Boccella, S., Belardo, C., Iannotta, M., Infantino, R., Formato, F., Marabese, I., Luongo, L., de Novellis, V., Maione, S., 2020. Behavioral, biochemical and electrophysiological changes in spared nerve injury model of neuropathic pain. Int. J. Mol. Sci. 21 (9), 3396. https://doi.org/10.3390/ijms21093396.
Guida, F., Iannotta, M., Misso, G., Ricciardi, F., Boccella, S., Tirino, V., Falco, M., Desiderio, V., Infantino, R., Pieretti, G., de Novellis, V., Papaccio, G., Luongo, L., Caraglia, M., Maione, S., 2022. Long-term neuropathic pain behaviors correlate with synaptic plasticity and limbic circuit alteration: a comparative observational study in mice. Pain 163 (8), 1590. https://doi.org/10.1097/j.pain.0000000000002549.
Hegyi, Z., Oláh, T., Kőszeghy, Á., Piscitelli, F., Holló, K., Pál, B., Csernoch, L., Di Marzo, V., Antal, M., 2018. CB1 receptor activation induces intracellular Ca2+ mobilization and 2-arachidonoylglycerol release in rodent spinal cord astrocytes. Sci. Rep. 8 (1), 10562. https://doi.org/10.1038/s41598-018-28763-6.
Imperatore, R., Morello, G., Luongo, L., Taschler, U., Romano, R., De Gregorio, D., Belardo, C., Maione, S., Di Marzo, V., Cristino, L., 2015. Genetic deletion of monoacylglycerol lipase leads to impaired cannabinoid receptor CB $_1$ R signaling and anxiety-like behavior. J. Neurochem. 135 (4), 799–813. https://doi.org/10.1111/jnc.13267.
Izzo, A.A., Borrelli, F., Capasso, R., Di Marzo, V., Mechoulam, R., 2009. Non-psychotropic plant cannabinoids: new therapeutic opportunities from an ancient herb. Trends Pharmacol. Sci. 30 (10), 515–527. https://doi.org/10.1016/j.tips.2009.07.006.
Jay, T.M., Zilkha, E., Obrenovitch, T.P., 1999. Long-term potentiation in the dentate gyrus is not linked to increased extracellular glutamate concentration. J. Neurophysiol. 81 (4), 1741–1748. https://doi.org/10.1152/jn.1999.81.4.1741.
Kędziora, M., Boccella, S., Marabese, I., Mlost, J., Infantino, R., Maione, S., Starowicz, K., 2023. Inhibition of anandamide breakdown reduces pain and restores LTP and monoamine levels in the rat hippocampus via the CB_1 receptor following osteoarthritis. Neuropharmacology. 222, 109304. doi: 10.1016/j.neuropharm.2022.109304. Epub 2022 Oct 28.
Leinen, Z.J., Mohan, R., Premadasa, L.S., Acharya, A., Mohan, M., Byrareddy, S.N., 2023. Therapeutic potential of Cannabis: a comprehensive review of current and future applications. Biomedicines 11 (10), 2630. https://doi.org/10.3390/biomedicines11102630.
Lorente, J.D., Cuitavi, J., Rullo, L., Candeletti, S., Romualdi, P., Hipólito, L., 2024. Sex-dependent effect of inflammatory pain on negative affective states is prevented by kappa opioid receptors blockade in the nucleus accumbens shell. Neuropharmacology 242, 109764. https://doi.org/10.1016/j.neuropharm.2023.109764.
Malvestio, R.B., Medeiros, P., Negrini-Ferrari, S.E., Oliveira-Silva, M., Medeiros, A.C., Padovan, C.M., Luongo, L., Maione, S., Coimbra, N.C., de Freitas, R.L., 2021. Cannabidiol in the prelimbic cortex modulates the comorbid condition between the chronic neuropathic pain and depression-like behaviour in rats: the role of medial prefrontal cortex 5-HT1A and CB1 receptors. Brain Res. Bull. 174, 323–338. https://doi.org/10.1016/j.brainresbull.2021.06.017.
Mannucci, C., Navarra, M., Calapai, F., Spagnolo, E.V., Busardò, F.P., Cas, R.D., Ippolito, F.M., Calapai, G., 2017. Neurological aspects of medical use of cannabidiol. CNS Neurol. Disord. - Drug Targets 16 (5), 541–553. https://doi.org/10.2174/1871527316666170413114210.
Manzanares, J., Corchero, J., Romero, J., Fernández-Ruiz, J.J., Ramos, J.A., Fuentes, J. A., 1999. Pharmacological and biochemical interactions between opioids and cannabinoids. Trends Pharmacol. Sci. 20 (7), 287–294. https://doi.org/10.1016/s0165-6147(99)01339-5.
Mason, D.J., Lowe, J., Welch, S.P., 1999. Cannabinoid modulation of dynorphin A: correlation to cannabinoid-induced antinociception. Eur. J. Pharmacol. 378 (3), 237–248. https://doi.org/10.1016/S0014-2999(99)00479-3.
Massotte, D., 2015. *In vivo* opioid receptor heteromerization: where do we stand? Br. J. Pharmacol. 172 (2), 420–434. https://doi.org/10.1111/bph.12702.
McCurdy, C.R., Sufka, K.J., Smith, G.H., Warnick, J.E., Nieto, M.J., 2006. Antinociceptive profile of salvinorin A, a structurally unique kappa opioid receptor agonist. Pharmacol. Biochem. Behav. 83 (1), 109–113. https://doi.org/10.1016/j.pbb.2005.12.011.
Medeiros, A.C., Medeiros, P., Pigatto, G.R., Maione, S., Coimbra, N.C., de Freitas, R.L., 2024. Cannabidiol in the dorsal hippocampus attenuates emotional and cognitive impairments related to neuropathic pain: role of prelimbic neocortex-hippocampal connections. Prog. Neuro Psychopharmacol. Biol. Psychiatr., 111039 https://doi.org/10.1016/j.pnpbp.2024.111039.
Messersmith, D.J., Kim, D.J., Gu, J., Dubner, R., Iadarola, M.J., 1996. c-Jun activation of the DYNCRE3 site in the prodynorphin promoter. Brain Res Mol Brain Res 40 (1), 15–21. https://doi.org/10.1016/0169-328x(96)00029-0.
Messersmith, D.J., Kim, D.J., Iadarola, M.J., 1998. Transcription factor regulation of prodynorphin gene expression following rat hind paw inflammation. Brain Res Mol Brain Res 53 (1–2), 260–269. https://doi.org/10.1016/s0169-328x(97)00308-2.
Meunier, A., Latrémolière, A., Mauborgne, A., Bourgoin, S., Kayser, V., Cesselin, F., Hamon, M., Pohl, M., 2005. Attenuation of pain-related behavior in a rat model of trigeminal neuropathic pain by viral-driven enkephalin overproduction in trigeminal ganglion neurons. Mol. Ther. 11 (4), 608–616. https://doi.org/10.1016/j.ymthe.2004.12.011.
Nation, K.M., De Felice, M., Hernandez, P.I., Dodick, D.W., Neugebauer, V., Navratilova, E., Porreca, F., 2018. Lateralized kappa opioid receptor signaling from the amygdala central nucleus promotes stress-induced functional pain. Pain 159 (5), 919–928. https://doi.org/10.1097/j.pain.0000000000001167.
Navarro, M., Carrera, M.R.A., Fratta, W., Valverde, O., Cossu, G., Fattore, L., Chowen, J. A., Gómez, R., Del Arco, I., Villanúa, M.A., Maldonado, R., Koob, G.F., De Fonseca, F. R., 2001. Functional interaction between opioid and cannabinoid receptors in drug self-administration. J. Neurosci. 21 (14), 5344–5350. https://doi.org/10.1523/JNEUROSCI.21-14-05344.2001.
Navratilova, E., Ji, G., Phelps, C., Qu, C., Hein, M., Yakhnitsa, V., Neugebauer, V., Porreca, F., 2019. Kappa opioid signaling in the central nucleus of the amygdala promotes disinhibition and aversiveness of chronic neuropathic pain. Pain 160 (4), 824–832. https://doi.org/10.1097/j.pain.0000000000001458.
Nguyen, C., Moeller, K.E., McGuire, M., Melton, B.L., 2023. Consumer perception, knowledge, and uses of cannabidiol. The Mental Health Clinician 13 (5), 217–224. https://doi.org/10.9740/mhc.2023.10.217.
Palazzo, E., Marabese, I., Luongo, L., Boccella, S., Bellini, G., Giordano, M.E., Rossi, F., Scafuro, M., de Novellis, V., Maione, S., 2013. Effects of a metabotropic glutamate receptor subtype 7 negative allosteric modulator in the periaqueductal grey on pain responses and rostral ventromedial medulla cell activity in rat. Mol. Pain 9. https://doi.org/10.1186/1744-8069-9-44, 1744-8069-9–44.
Pearl-Dowler, L., Posa, L., Lopez-Canul, M., Teggin, A., Gobbi, G., 2023. Anti-allodynic and medullary modulatory effects of a single dose of delta-9-tetrahydrocannabinol (THC) in neuropathic rats tolerant to morphine. Prog. Neuro-Psychopharmacol. Biol. Psychiatry 127, 110805. https://doi.org/10.1016/j.pnpbp.2023.110805.
Piscitelli, F., Guida, F., Luongo, L., Iannotti, F.A., Boccella, S., Verde, R., Lauritano, A., Imperatore, R., Smoum, R., Cristino, L., Lichtman, A.H., Parker, L.A., Mechoulam, R., Maione, S., Di Marzo, V., 2020. Protective effects of *N* -oleoylglycine in a mouse model of mild traumatic brain injury. ACS Chem. Neurosci. 11 (8), 1117–1128. https://doi.org/10.1021/acschemneuro.9b00633.
Rahn, E.J., Guzman-Karlsson, M.C., David Sweatt, J., 2013. Cellular, molecular, and epigenetic mechanisms in non-associative conditioning: implications for pain and memory. Neurobiol. Learn. Mem. 105, 133–150. https://doi.org/10.1016/j.nlm.2013.06.008.
Ren, K., Dubner, R., 1999. Inflammatory models of pain and hyperalgesia. ILAR J. 40 (3), 111–118. https://doi.org/10.1093/ilar.40.3.111.
Ross, B., Trojian, T., Cushman, D.M., 2023. Physician perceptions of cannabidiol (CBD) and Cannabis in sports medicine and performance. Translational Sports Medicine 2023, e8824466. https://doi.org/10.1155/2023/8824466.
Saffarpour, S., Shaabani, M., Naghdi, N., Farahmandfar, M., Janzadeh, A., Nasirinezhad, F., 2017. In vivo evaluation of the hippocampal glutamate, GABA and the BDNF levels associated with spatial memory performance in a rodent model of

neuropathic pain. Physiol. Behav. 175, 97–103. https://doi.org/10.1016/j.physbeh.2017.03.025.

Saviano, A., Raucci, F., Tallarico, M., De Caro, C., Di Martino, S., Nesci, V., Roberti, R., Iannone, L.F., Colia, A.L., Dimonte, S., 2021. Cannabidiol and the central nervous system: translating into clinics. Pharm. Adv 3, 369.

Scarante, F.F., Ribeiro, M.A., Almeida-Santos, A.F., Guimarães, F.S., Campos, A.C., 2021. Glial cells and their contribution to the mechanisms of action of cannabidiol in neuropsychiatric disorders. Front. Pharmacol. 11. https://doi.org/10.3389/fphar.2020.618065.

Scavone, J.L., Sterling, R.C., Van Bockstaele, E.J., 2013. Cannabinoid and opioid interactions: implications for opiate dependence and withdrawal. Neuroscience 248, 637–654. https://doi.org/10.1016/j.neuroscience.2013.04.034.

Schuele, L.-L., Schuermann, B., Bilkei-Gorzo, A., Gorgzadeh, S., Zimmer, A., Leidmaa, E., 2022. Regulation of adult neurogenesis by the endocannabinoid-producing enzyme diacylglycerol lipase alpha (DAGLa). Sci. Rep. 12 (1), 633. https://doi.org/10.1038/s41598-021-04600-1.

Sim-Selley, L.J., 2003. Regulation of cannabinoid CB1 receptors in the central nervous system by chronic cannabinoids. Crit. Rev. Neurobiol. 15 (2), 91–119. https://doi.org/10.1615/CritRevNeurobiol.v15.i2.10.

Sim-Selley, L.J., Schechter, N.S., Rorrer, W.K., Dalton, G.D., Hernandez, J., Martin, B.R., Selley, D.E., 2006. Prolonged recovery rate of CB_1 receptor adaptation after cessation of long-term cannabinoid administration. Mol. Pharmacol. 70 (3), 986–996. https://doi.org/10.1124/mol.105.019612.

Tucci, P., Mhillaj, E., Morgese, M.G., Colaianna, M., Zotti, M., Schiavone, S., Cicerale, M., Trezza, V., Campolongo, P., Cuomo, V., Trabace, L., 2014. Memantine prevents memory consolidation failure induced by soluble beta amyloid in rats. Front. Behav. Neurosci. 8. https://doi.org/10.3389/fnbeh.2014.00332.

Vučković, S., Srebro, D., Vujović, K.S., Vučetić, Č., Prostran, M., 2018. Cannabinoids and pain: new insights from old molecules. Front. Pharmacol. 9, 1259. https://doi.org/10.3389/fphar.2018.01259.

Wang, Z., Gardell, L.R., Ossipov, M.H., Vanderah, T.W., Brennan, M.B., Hochgeschwender, U., Hruby, V.J., Malan Jr., T.P., Lai, J., Porreca, F., 2001. Pronociceptive actions of dynorphin maintain chronic neuropathic pain. J. Neurosci. 21 (5), 1779–1786. https://doi.org/10.1523/JNEUROSCI.21-05-01779.2001.

Wang, Y.-J., Hang, A., Lu, Y.-C., Long, Y., Zan, G.-Y., Li, X.-P., et al., 2016. κ Opioid receptor activation in different brain regions differentially modulates anxiety-related behaviors in mice. Neuropharmacology 110, 92–101.

Welch, S.P., 2009. Interaction of the cannabinoid and opioid systems in the modulation of nociception. Int. Rev. Psychiatr. 21 (2), 143–151. https://doi.org/10.1080/09540260902782794.

Wu, Z., Guo, Z., Gearing, M., Chen, G., 2014. Tonic inhibition in dentate gyrus impairs long-term potentiation and memory in an Alzheimer's disease model. Nat. Commun. 5 (1), 4159. https://doi.org/10.1038/ncomms5159.

Xu, M., Petraschka, M., McLaughlin, J.P., Westenbroek, R.E., Caron, M.G., Lefkowitz, R. J., Czyzyk, T.A., Pintar, J.E., Terman, G.W., Chavkin, C., 2004. Neuropathic pain activates the endogenous kappa opioid system in mouse spinal cord and induces opioid receptor tolerance. J. Neurosci. 24 (19), 4576–4584. https://doi.org/10.1523/JNEUROSCI.5552-03.2004.

Zamberletti, E., Piscitelli, F., De Castro, V., Murru, E., Gabaglio, M., Colucci, P., Fanali, C., Prini, P., Bisogno, T., Maccarrone, M., Campolongo, P., Banni, S., Rubino, T., Parolaro, D., 2017. Lifelong imbalanced LA/ALA intake impairs emotional and cognitive behavior via changes in brain endocannabinoid system. JLR (J. Lipid Res.) 58 (2), 301–316. https://doi.org/10.1194/jlr.M068387.